

ARCHAEOLOGICAL INVESTIGATIONS OF STONE DETERIORATION IN  
KALECIK (ANKARA) CASTLE

A THESIS SUBMITTED TO  
THE GRADUATE SCHOOL OF NATURAL AND APPLIED SCIENCES  
OF  
MIDDLE EAST TECHNICAL UNIVERSITY

BY

ALP OSMAN AKOĞLU

IN PARTIAL FULFILLMENT OF THE REQUIREMENTS  
FOR  
THE DEGREE OF MASTER OF SCIENCE  
IN  
ARCHAEOLOGY

FEBRUARY 2012

Approval of the thesis:

ARCHAEOLOGICAL INVESTIGATIONS OF STONE DETERIORATION IN  
KALECIK (ANKARA) CASTLE

submitted by **ALP OSMAN AKOĞLU** in partial fulfillment of the requirements for  
the degree of **Master of Science in Department of Archaeometry, Middle East  
Technical University** by,

Prof. Dr. Canan Özgen  
Dean, Graduate School of **Natural and Applied Sciences**

Prof. Dr. Ümit M. Atalay  
Head of Department, **Archaeometry**

Prof. Dr. Tamer Topal  
Supervisor, **Geological Engineering Dept., METU**

Prof. Dr. Ömür Bakırer  
Co-Supervisor, **Architecture Dept., METU**

**Examining Committee Members:**

Prof. Dr. Asuman G. Türkmenoğlu  
Geological Engineering Dept., METU

Prof. Dr. Tamer Topal  
Geological Engineering Dept., METU

Prof. Dr. Emine Caner-Saltık  
Architecture Dept., METU

Prof. Dr. Ömür Bakırer  
Architecture Dept., METU

Prof. Dr. Şahinde Demirci  
Chemical Engineering Dept., METU

**Date:**

**I hereby declare that all information in this document has been obtained and presented in accordance with academic rules and ethical conduct. I also declare that, as required by these rules and conduct, I have fully cited and referenced all material and results that are not original to this work.**

Name, Last name: Alp Osman Akođlu

Signature :

## **ABSTRACT**

### **ARCHAEOOMETRIC INVESTIGATIONS OF STONE DETERIORATION IN KALECIK (ANKARA) CASTLE**

Akođlu, Alp Osman

M.Sc, Department of Archaeometry

Supervisor : Prof. Dr. Tamer Topal

Co-Supervisor : Prof. Dr. Ömür Bakırer

February 2012, 61 pages

Kalecik Castle is an important historical building. However, dacitic building stone used is deteriorating mainly because of atmospheric conditions. The purpose of this study is to understand the deterioration mechanisms affecting the dacitic stones used in the castle's walls. To achieve this purpose various arhaeometrical methods such as petrography, X-ray diffraction analyses, analyses for determining physical properties (density, porosity, and water absorption capacities), ultrasonic velocity measurements and some mechanical tests are used.

The results of this study show that the deterioration of Kalecik Castle results mostly from physical factors such as frost action, wetting and drying and thermal shock. According to the study, chemical and biological factors that may also be an important cause of deterioration are negligible in Kalecik Castle's building stones.

Keywords: Dacite, Kalecik Castle, Stone Deterioration

## ÖZ

### KALECİK (ANKARA) KALESİNDEKİ TAŞ BOZULMASININ ARKEOMETRİK İNCELEMESİ

Akođlu, Alp Osman

Yüksek Lisans, Arkeometri Bölümü

Tez Yöneticisi : Prof. Dr. Tamer Topal

Ortak Tez Yöneticisi : Prof. Dr. Ömür Bakırer

Şubat 2012, 61 sayfa

Kalecik Kalesi önemli bir tarihi yapıdır. Ne var ki kalede yapı taşı olarak kullanılan dasit taşlar temelde atmosfer koşullarına bađlı olarak bozulmaktadır. Bu çalışmanın amacı kalenin yapı taşlarının bozulmasına yol açan mekanizmaları ortaya çıkarmaktır. Buna yönelik olarak petrografi, X-ışını difraktometrisi, fiziksel özellikleri tespit etmeye yönelik analizler (yođunluk, gözeneklilik, su emme kapasitesi), ultrasonik hız ölçümleri ve birtakım mekanik testler gibi çeşitli arkeometrik yöntemlerden yararlanılmıştır.

Bu çalışma Kalecik Kalesi'ni oluşturan taşların önemli ölçüde donma/erime, ıslanma/kuruma ve ısı şok gibi fiziksel etkilerle bozulduđunu göstermektedir. Yine bu çalışmaya göre taş bozulmasında önemli rol oynayabilen kimyasal ve biyolojik etkiler Kalecik Kalesi'ndeki taş bozulmasında ihmal edilebilecek düzeydedir.

Anahtar Kelimeler: Dasit, Kalecik Kalesi, Taş Bozulması

To My Family...

## ACKNOWLEDGEMENT

I would like to thank my thesis supervisor Prof. Dr. Tamer Topal for his supervision and moral guidance. Without his guidance and understanding this study would not be accomplished.

It would like to express my gratitude to Prof. Dr. Emine Caner-Saltık for encouraging me to return to the department, her supervision, enabling and encouraging me to use the equipment and the resources in Materials Conservation Laboratory.

I would like to express my special thanks to Şenay Dinçer, Dr. Göze Akoğlu, Dr. Alp Güney and other researchers in the Materials Conservation Laboratory for their help and guidance during laboratory experiments.

My special thanks are to Talia Yaşar for sparing her time and for her invaluable support during thin section analyses.

I would also like to thank Dr. Kaan Sayit for his help in thin section analyses.

I am grateful to my family and my friends for their support throughout the study.

## TABLE OF CONTENTS

ABSTRACT .....	iv
ÖZ .....	v
ACKNOWLEDGEMENTS .....	vii
TABLE OF CONTENTS .....	viii
LIST OF TABLES .....	x
LIST OF FIGURES .....	xi
CHAPTERS	
1. INTRODUCTION .....	1
1.1. Scope of the Study .....	1
1.2. Location of the Study Area .....	2
1.3. Kalecik in History .....	3
1.4. Kalecik Castle .....	4
1.4.1. Restoration of the Castle in 2007 .....	6
1.5. Geology of the Region .....	8
1.6. The Material .....	10
2. WEATHERING OF STONE .....	12
2.1. Chemical Weathering .....	13
2.2. Physical Weathering .....	14
2.3. Biological Weathering .....	16
3. MATERIALS AND METHODS .....	18
3.1. Description of Samples .....	18
3.2. Thin Section Analyses .....	20
3.3. X-Ray Powder Diffraction Analyses .....	20
3.3.1. Unoriented XRD Sample Preparation and Methodology .....	20
3.3.2. Oriented XRD Sample Preparation and Methodology .....	21
3.4. Basic Physical Properties .....	24
3.4.1. Porosity .....	25



3.4.2. Bulk Density .....	25
3.4.3. Water Absorption Capacity .....	25
3.5. Ultrasonic Pulse Velocity Measurements .....	26
3.6. Modulus of Elasticity .....	28
3.7. Durability Tests.....	29
4. EXPERIMENTAL RESULTS .....	30
4.1. Thin Section Analyses .....	30
4.2. X-Ray Powder Diffraction Analyses .....	34
4.3. Basic Physical Properties .....	35
4.3.1. Porosities .....	36
4.3.2. Bulk Densities .....	36
4.3.3. Water Absorption Capacities.....	36
4.4. Ultrasonic Pulse Velocity Measurements .....	37
4.4.1. Direct Measurements.....	37
4.4.1. Indirect Measurements from Surface (Exterior) .....	38
4.4.1. Indirect Measurements from Surface (Interior).....	39
4.4.1. Indirect Measurements with one Probe Fixed.....	40
4.5. Modulus of Elasticity .....	42
4.6. Durability Tests.....	43
5. CONCLUSIONS .....	47
REFERENCES.....	50
APPENDIX.....	52
X-RAY POWDER DIFFRACTION CHARTS .....	52

## LIST OF TABLES

### TABLES

<b>Table 1</b>	Summary of the properties of samples prepared from each stone .....	21
<b>Table 2</b>	Calculated porosities of samples .....	35
<b>Table 3</b>	Calculated bulk densities of samples .....	36
<b>Table 4</b>	Calculated porosities of samples .....	37
<b>Table 5</b>	Ultrasonic pulse velocities in samples (direct measurement) .....	38
<b>Table 6</b>	Ultrasonic pulse velocities in samples (indirect measurement from the surface).....	38
<b>Table 7</b>	Ultrasonic pulse velocities in samples (indirect measurement from the inside).....	39
<b>Table 8</b>	Indirect ultrasonic velocity measurements with one probe fixed for Stone 1 .....	40
<b>Table 9</b>	Indirect ultrasonic velocity measurements with one probe fixed for Stone 4 .....	41
<b>Table 10</b>	Indirect ultrasonic velocity measurements with one probe fixed for Stone 5 .....	41
<b>Table 11</b>	Modulus of elasticity calculations for stone samples.....	42
<b>Table 12</b>	Changes in samples after repeated freeze/thaw cycles.....	43
<b>Table 13</b>	Changes in samples after repeated salt crystallization cycles .....	43
<b>Table 14</b>	Changes in unconfined compressive strength / porosity ratios after repeated cycles .....	44

## LIST OF FIGURES

### FIGURES

<b>Figure 1</b> Location of Kalecik in Ankara / Turkey.....	2
<b>Figure 2</b> Kalecik Castle as seen from south.....	5
<b>Figure 3</b> Deterioration in restored stone.....	6
<b>Figure 4</b> Deterioration in natural stone forming the base of the castle.....	6
<b>Figure 5</b> Restored walls of the castle.....	7
<b>Figure 6</b> Geological map of the region.....	8
<b>Figure 7</b> QAPF Diagram of volcanic rocks.....	10
<b>Figure 8</b> Lichen covered and deteriorated surface of Stone 2.....	19
<b>Figure 7</b> Cut surface of Stone 5.....	19
<b>Figure 10</b> Deteriorated and flaked surface of Stone 4.....	22
<b>Figure 11</b> Deteriorated and flaked surface of Stone 5.....	23
<b>Figure 12</b> Thin section photograph from Stone 1 showing a large quartz phenocrystal and a large glomeroporphyritic plagioclase phenocrystal ...	31
<b>Figure 13</b> A large plagioclase phenocrystal having sieve texture.....	32
<b>Figure 14</b> Carbonate filling in one of the fractures in Stone 5.....	33
<b>Figure 15</b> X-ray powder diffraction plot of powder sample prepared from Stone 1.....	34
<b>Figure 16</b> Porosity comparison of each sample's fresh and deteriorated parts.....	35
<b>Figure 17</b> Bulk density comparison of each sample's fresh and deteriorated parts ..	36
<b>Figure 18</b> Water absorption capacity comparison of each sample's fresh and deteriorated parts.....	37
<b>Figure 19</b> Ultrasonic pulse velocities in samples (direct measurement).....	38
<b>Figure 20</b> Ultrasonic pulse velocities in samples (indirect measurement).....	39
<b>Figure 21</b> Ultrasonic pulse velocities in samples (indirect measurement from the inside).....	39
<b>Figure 22</b> Indirect ultrasonic velocity measurements with one probe fixed for Stone 1.....	40
<b>Figure 23</b> Indirect ultrasonic velocity measurements with one probe fixed for Stone 4.....	41

<b>Figure 24</b> Indirect ultrasonic velocity measurements with one probe fixed for Stone 5.....	42
<b>Figure 25</b> Modulus of elasticity calculations for stone samples .....	42
<b>Figure 26</b> Change in dry densities after repeated freeze/thaw and salt crystallization cycles .....	44
<b>Figure 27</b> Change in saturated densities after repeated freeze/thaw and salt crystallization cycles .....	44
<b>Figure 28</b> Change in porosities after repeated freeze/thaw and salt crystallization cycles .....	45
<b>Figure 29</b> Change in porosity after repeated freeze/thaw and salt crystallization cycles under atmospheric pressure .....	45
<b>Figure 30</b> Change in saturated densities after repeated freeze/thaw and salt crystallization cycles under atmospheric pressure .....	45
<b>Figure 31</b> Change in dry densities after repeated freeze/thaw and salt crystallization cycles under atmospheric pressure .....	46
<b>Figure 32</b> Change in water absorption capacities after repeated freeze/thaw and salt crystallization cycles .....	46
<b>Figure 33</b> Change in water absorption capacities after repeated freeze/thaw and salt crystallization cycles under atmospheric pressure .....	46
<b>Figure 34</b> X-ray diffraction chart for samples collected from the interior parts of Stone 1 .....	52
<b>Figure 35</b> X-ray diffraction chart for samples collected from the surface of Stone 1.....	53
<b>Figure 36</b> X-ray diffraction chart for samples collected from the ground mass of Stone 1 .....	53
<b>Figure 37</b> X-ray diffraction chart for samples collected from the interior parts of Stone 2 .....	54
<b>Figure 38</b> X-ray diffraction chart for samples collected from the surface of Stone 2.....	54
<b>Figure 39</b> X-ray diffraction chart for samples collected from the interior parts of Stone 3 .....	55
<b>Figure 40</b> X-ray diffraction chart for samples collected from the interior parts of Stone 4 .....	56
<b>Figure 41</b> X-ray diffraction chart for samples collected from the surface of Stone 4.....	56
<b>Figure 42</b> X-ray diffraction chart for samples collected from the interior parts of Stone 5 .....	57
<b>Figure 43</b> X-ray diffraction chart for samples collected from surface of Stone 5 ....	57

<b>Figure 44</b> Oriented X-ray diffraction charts for samples collected from 5 cm beneath the surface of Stone 1 .....	58
<b>Figure 45</b> Oriented X-ray diffraction charts for samples collected from near surface of Stone 1 .....	59
<b>Figure 46</b> Oriented X-ray diffraction charts for samples collected from flaked parts of Stone 2 .....	60
<b>Figure 47</b> Oriented X-ray diffraction charts for samples scratched from the surface of Stone 5 .....	61

# CHAPTER 1

## INTRODUCTION

### 1.1. Scope of the Study

Kalecik Castle which gives its name to Kalecik town is an important Roman Period historical heritage. Although the “cik” suffix added to “Kale” (which means Castle) may evoke that the castle is a small structure, the dimensions of the castle measure about 170 to 100 meters and it is built on a monumental volcanic cone in the middle of the Kalecik town. The castle is the symbol of the town and one of the most important historical structures in Kalecik and Ankara.

The Kalecik Castle was largely ruined by the year 2007. Especially the western and northern parts of the walls were ruined almost completely. The castle is built from the dacitic stones gathered from the volcanic cone where the castle sits on. The building stones of the castle were deteriorated heavily which may be the leading reason for the falling down of the walls.

Kalecik Municipality restored the castle in 2007. The ruined parts of the castle walls, ramparts and bastions were erected completely during this restoration study. The surfaces of remainings or previously restored parts of the walls were also cleaned. Today, most of the castle looks in pretty good condition. But the rocks forming the base of the castle are still largely deteriorated in the form of spalling, and the restored and cleaned stones are now subjected to deterioration.

The purpose of this study is to understand the deterioration mechanisms of the stones used in the Kalecik Castle’s walls. To achieve this purpose various arhaeometrical methods are used. This study may also help to understand the properties of the

dacitic stone in the region. This may be important because the stones mined from this region are used as building stones in most of the historical buildings like mosques, old houses, public buildings, bridges, etc. in Kalecik. It is easy to see the deteriorated surfaces in these buildings too. The author of this study hopes that the results of this study would be useful for the future restoration and preservation studies to be carried on these buildings.

## **1.2. Location of the Study Area**

Kalecik being a district of Ankara is a town located at 67 km northeast of the city (Figure 1). Kalecik is founded near the plain land around the longest river of Turkey, Kızılırmak. It covers an area of 1340 km<sup>2</sup>, and the average elevation is about 725 m.

The highest peak in Kalecik is İdris Dağı (1992 m) which is located at the west of the district. Kalecik is surrounded by Bozkır Dağı (1117 m) at north, Karagüney Dağı (1226 m) at east and south. According to the 2010 census, population of the district is 14,517 of which 9450 live in the town of Kalecik.

The study area is a dome shaped volcanic cone, which has a height of about 150 m. The Kalecik district is settled around, especially at the north east of the hill. Kalecik castle is built on this hill.

Kalecik is located at the northwestern part of the Central Anatolian geographical region. Central Anatolia has a semi-arid continental climate. The summers are hot and dry, the winters are cold and snowy. The region has low precipitation throughout the year. Because of the milder effect of the Kızılırmak River and being surrounded by hills, summers are hot and winters are mild in Kalecik. However, the annual rainfall is quite low. Kalecik has a microclimate which enables a wider variety of vegetation to be grown. Among these, Kalecik Karası is one of the prestigious wine grape varieties used for wine production.



**Figure 1** Location of Kalecik in Ankara / Turkey

### **1.3. Kalecik in History**

Kalecik and the surrounding region were an important settlement area since Hittite period and occupied by Hittites until the end of Hittite Empire. After the collapse of the Hittite Empire at the beginning of the 12th century BC, the Phrygians established their kingdom with a capital eventually at Gordium.

Phrygians dominated the Kalecik area until 550 BC and Phrygia passed under Persian dominion. In 334 BC Alexander the Great invaded Asia Minor. He broke the power of Persia in a series of battles and then conquered the entire Persian Empire. After the death of Alexander the Great in 323 BC, the area was invaded by the Gallians.

After the Gallians, the Roman Empire dominated Anatolia for about 400 years, Roman Empire was divided into two and Eastern Roman Empire was named Byzantine Empire. Some remains were found dating to these periods at the excavations made around the region. The ruins or the ancient structures especially dated to Roman and Byzantine periods lead to the conclusion that Kalecik was an important settlement area during these periods (Aslangil and Ekiz, 1996).



In Evliya Çelebi's travel notes named "Seyahatname" Çelebi noted that Kalecik Castle was built in the Roman period by a Bursa feudal landlord as a dowry to his daughter (Aslangil and Ekiz, 1996).

After Malazgirt War in 1071, Turks entered Anatolia and Byzantines gradually receded from Anatolia. Kalecik is said to be conquered from the Byzantines by the Turks led by Seydi Battal Gazi in 1075.

For a short period during the Seljuqs of Rum (Anadolu Selçukluları) Sultan Ghiyath al-Din Kaykhusraw II (Giyaseddin Keyhüsrev) (1237-1246), the Kalecik region was invaded by the Mongolians (Aslangil and Ekiz, 1996).

In 1255, the Mongols invaded the central and eastern Anatolia, and remained there until 1335. The Seljuk State split into small emirates and rescued themselves from both Mongol and Seljuk control. By the end of the 14<sup>th</sup> century, various beyliks were controlling most of. The Turkmens were under the control of the Mongols.

The Ilkhanates was stationed near Ankara. After the decline of the Ilkhanates, the Mongol Empire's legacy was overthrown by Kadi Burhan al-Din in the late 14<sup>th</sup> century.

Ottomans, one of the Turkmen beyliks emerged as great power under Osman and his son Orhan. Ottomans absorbed all of the Anatolian beyliks during the 15th century. During the Ottoman Empire, a popular fabric named "Ankara sofı" was being weaved in Kalecik and around to be used as a dress. Kalecik was a developed trade center of the times and it was known as "Little Egypt" (Aslangil and Ekiz, 1996).

#### **1.4. Kalecik Castle**

The Castle is located at the center to east of the Kalecik settlement. This Roman period heritage is built on a steep rock mass (hill) about 150 meters high (Figure 2).

The walls of the castle were built from dacite stones which was largely deteriorated (Figures 3 and 4) and ruined by the year 2007. Especially the western and northern

parts of the castle walls were ruined almost completely. The ruins of these walls are probably dated to the first building period of the castle. The eastern walls had undergone some restorations in the past. The heights of the eastern walls are between 11 to 12 meters. The thickness of the walls varies between 0.7 and 1 meters.



**Figure 2** Kalecik Castle as seen from south

The walls of the castle is built from roughly cut prismatic stones and their sizes vary to a great extent. The lengths of the long sides of the prismatic stones are 10 to 50 centimeters. The stones forming the walls are mostly arranged in rows but at some parts of the walls, irregular shaped stones are used. The foundation of the castle is mostly made of rough stones and they are generally arranged irregularly.

In their book about Kalecik's History, Halit Cevri Aslangil and Halil Hamdi Ekiz describe the castle as follows:

The entrance of the castle is an arched doorway and there are two cylindrical towers at both side of the gate. The castle includes a large chamber located about 20 meters from the center of the castle, and there is a square shaped opening at the top. Today, most of the chamber is filled with rubble. It is assumed that this chamber is used as a cistern to provide water to the people settled in and around the castle (Aslangil and

Ekiz, 1996). Near the cistern, there is another room used as a tomb. The room is built with irregular shaped stones and lime mortar. The ceiling of this chamber is in the form of vault. The walls are covered with plaster but today they are mostly ruined (Aslangil and Ekiz, 1996).

Viewed from the south, there is a tunnel opening at the base of the outer walls. Today the tunnel has collapsed but it is thought that ancient people used this tunnel as a path to the Kızılırmak River to deliver water (Aslangil and Ekiz, 1996).

#### **1.4.1. Restoration of the Castle in 2007**

The Kalecik Municipality had restored the castle in 2007. According to the information provided from the contractor company (EG Mimarlık, 2011) who made the restoration, the ruined parts of the castle walls, ramparts and bastions were erected completely. The surfaces of the remaining or previously restored parts of the walls were also cleaned.



**Figure 3** Restorated southern walls of the castle

The completely ruined walls were rebuilt carefully where the bases of the walls were remaining (Figure 3). The stones used in the restoration were gathered from the region forming the foundation of the castle. No cement or derivatives were used in mortar of the restoration project. Instead, the restoration was made by using Horasan Mortar (a mixture of crumbs of bricks and tiles mixed with lime and some organic materials like egg yolk, milk, animal hair, etc. (Böke et al., 2004).



**Figure 4** Deterioration in restored stone



**Figure 5** Deterioration in natural stone forming the base of the castle

### **1.5. Geology of the Region**

The volcanic rocks in the Kalecik region (Figure 6) are defined in the booklet given together with the geology map of MTA's Çankırı H30 section (Dönmez, 2010). According to this work the volcanics around the Kalecik belong to "dacitic Kalecik volcanics". They are defined as white, gray quartz, feldspar and hornblende phenocrystals bearing dacitic rocks. Kalecik volcanics are mainly found around Gökdere Village and Kalecik center (where the Kalecik castle is located). The hill in Kalecik center is a volcanic cone.

According to the petrographic investigation of the samples gathered from Gökdere region, the rocks have porphyritic (rock that has a distinct difference in the size of the crystals, with at least one group of crystals obviously larger than another group) structure composed of mainly quartz, feldspar, and hydrated amphiboles (Dönmez, 2010).

It is not possible to date the Kalecik volcanic directly since there is not enough evidence. Nevertheless, it is possible to compare with the nearby regional formations. The Early–Middle Miocene volcanics which are interbedded with the deposits of the Hançili formation crop out in four different regions, namely Elmadağ, Haymana-Polatlı, Çubuk and Kalecik. The volcanics of Elmadağ region include the andesitic and basaltic Elmadağ volcanics, dacitic Oğulbey volcanics, dacitic-rhyolitic Tohumlar volcanics and basaltic Evciler volcanics (Dönmez, 2009). The volcanics in the Haymana-Polatlı region are andesitic Yenice volcanics, andesitic Balkuyumcu volcanics, rhyolitic-dacitic Hisarlıkaya volcanics, andesitic, dacitic, rhyolitic Oyaca volcanics and basaltic Polatlı volcanics.

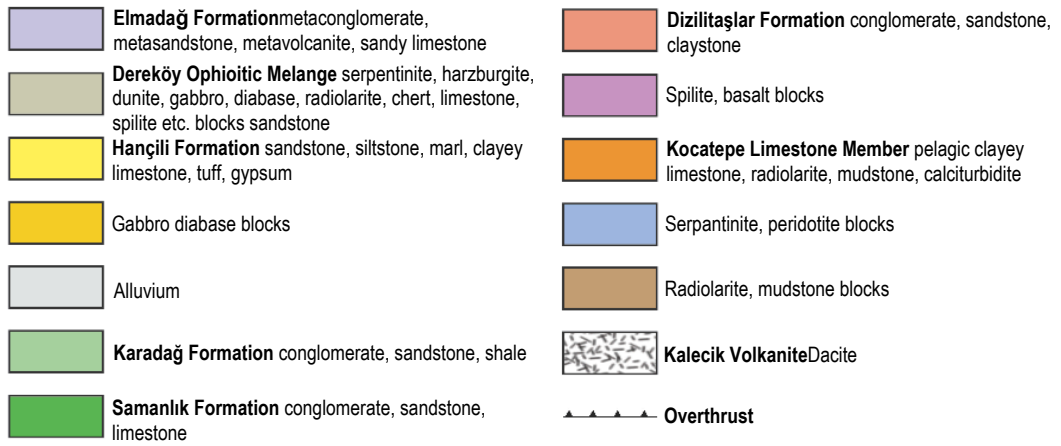
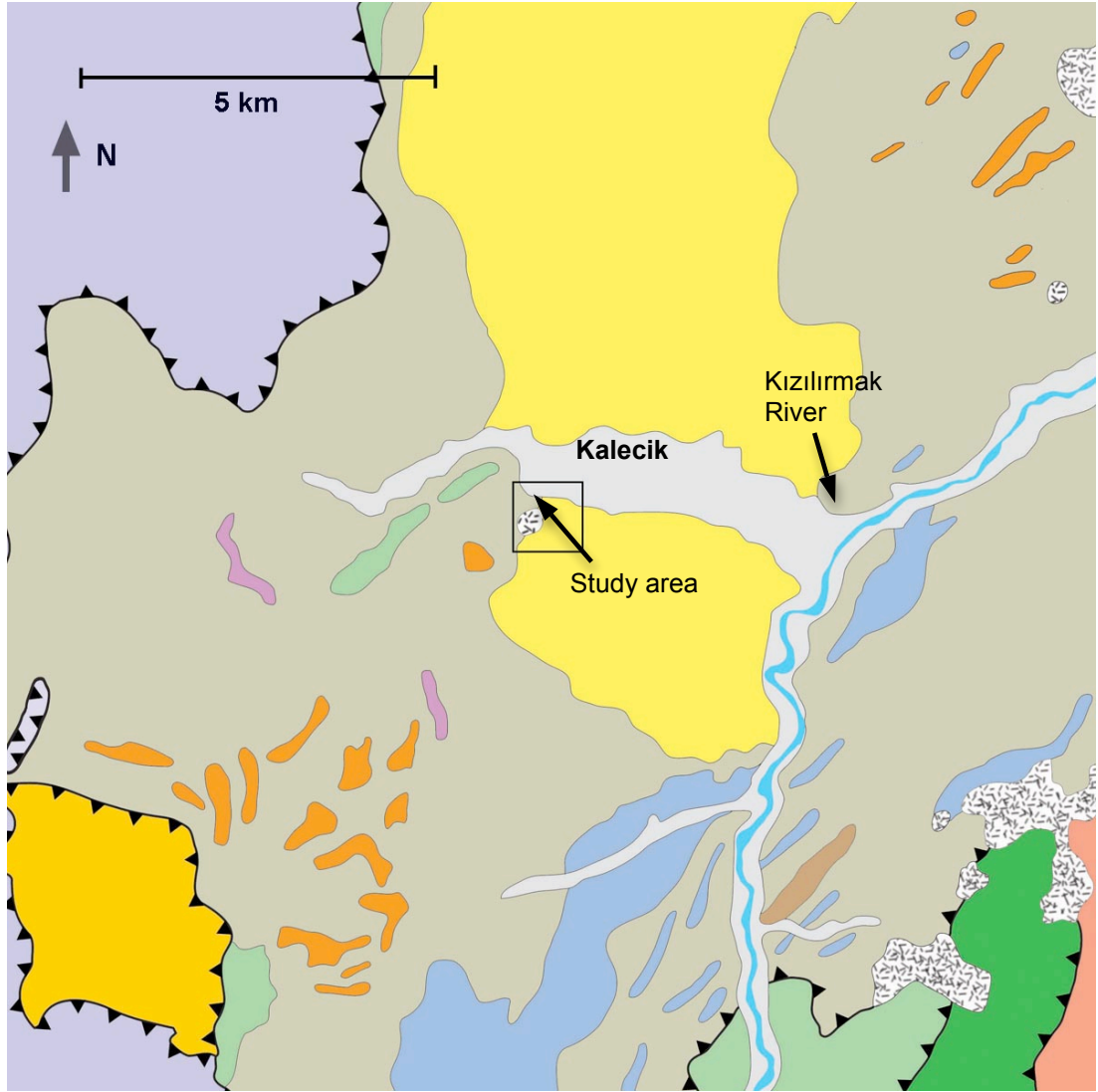


Figure 6 1/100.000 scaled geological map of the region (Dönmez, 2010)

## 1.6. The Material

The volcanics in the Kalecik region is dacitic Kalecik Volanics (Dönmez, 2009). The last volcanic activity in the area is represented by the olivine basaltic Evciler and Polatlı volcanics and the Aydos basalts. This activity lasted in different periods from Early Miocene onward and during Middle Miocene (Dönmez, 2009).

Dacite is a type of igneous rock consisting mostly of plagioclase feldspar with biotite, hornblende, and pyroxene. It has quartz as rounded, corroded phenocrystals. Quartz is also present in the ground-mass of the rock. According to the QAPF diagram (a double triangle diagram which is used to classify igneous rocks based on mineralogic composition where Q: Quartz, A: Alkali feldspar, P: Plagioclase, F: Feldspathoid) dacite may have a quartz ratio between 20% and 60% (Figure 7) (Blatt, 1996).

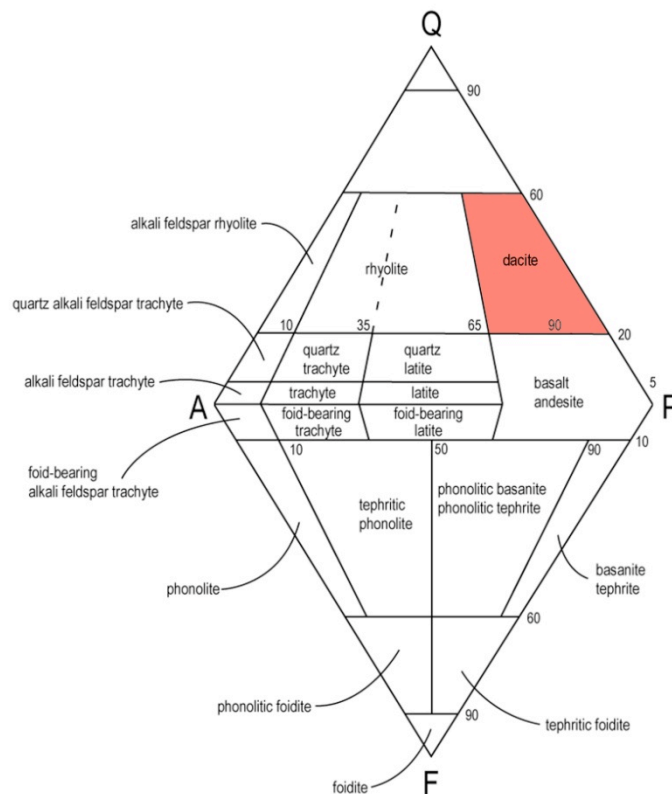


Figure 7 QAPF Diagram of volcanic rocks (Streckeisen, 1974)

In this study, according to the petrographic investigation there are very few number of quartz phenocrystals in the collected samples. The ground mass also contains quartz crystals although it is not possible to determine the exact percentage of quartz content by point counting precisely since the ground mass is composed of very small crystals.



## **CHAPTER 2**

### **WEATHERING OF STONE**

Rocks become stone when shaped by humans. Natural stone is used as a widespread building material since ancient times. It is also used for artistic medium such as sculptures. Even though stone is a cheap and very durable material, at least some types, it is subject to weathering in the long term. The deterioration of stone used in historical monuments and buildings is closely related to the geological processes of rock weathering.

Weathering is the breakdown and alteration of rocks. Rocks are usually preserved under the ground where the conditions are almost stable. Weathering usually starts when the rock faces atmosphere. The rocks start to alter when exposed to the unstable conditions of the atmosphere. Physical processes like temperature differences, eroding effects of rain and wind, frost, and chemical and biological factors fasten the deterioration processes. No weathering agent acts alone; the relative importance of each is influenced by the concurrent effect of other agents, or exposure to the action of one may render the material more susceptible to the subsequent action of another (Schaffer, 1972).

As a result of weathering processes, mineral particles like sand, silt, and clay are formed and this contributes to the formation of soil. Weathering processes extract elements and compounds from the rocks and these are used as nutrients by plants. The salt in the oceans and seas results from the release of ion salts from rocks and minerals on the land. Erosion and rivers transport these ions from land to the ocean basins. Weathering contributes to many other aspects of the hydrosphere, lithosphere

and biosphere. But also it is a main problem for the historical (recently made also) buildings and monuments.

There are three broad categories of mechanisms for weathering: chemical, physical and biological.

## **2.1. Chemical Weathering**

The chemical and mineralogical composition of the rocks may be altered by chemical processes. This occurs because of many different mechanisms. Hydrolysis Oxidation-reduction, hydration, carbonation, and solution are the most common chemical weathering processes (Pidwirny, 2006).

Hydrolysis involves the reaction between mineral ions and water. It results in the decomposition of the rock surface by forming new compounds. This process may increase pH of the solution. Hydrolysis is especially effective in the weathering of common silicate minerals (Pidwirny, 2006).

Oxidation occurs when compounds reacts with oxygen. Oxidized material gives electrons to oxygen and becomes less stable. Oxidation may cause the structures including these materials to become less rigid (Pidwirny, 2006).

Hydration involves inclusion of water into the structure. Hydration accelerates reactions by expanding the crystal lattice offering more surface area for reaction which speeds up decomposition (Pidwirny, 2006).

Carbonation is the reaction of carbonate and bicarbonate ions with minerals. The carbonates usually form as a result of other chemical processes. Carbon dioxide is the main cause of formation of carbonation. The amount of carbon dioxide is increasing gradually because of industrial activities and growing cities. This fastens the weathering processes especially buildings in the cities. Carbonic acid which is a product of carbon dioxide and water is an important cause of decomposition of mineral surfaces because of its acidic nature (Pidwirny, 2006).

Water is the most critical agent among the factors involved in stone weathering. Because stone is a porous material, in the presence of rain or moisture, water is absorbed into the stone by capillary action. Then, in dry weather the water evaporates back to the surface. Also, the flow of water outside the stone plays a role in weathering of stone (Dorsey et al., 1999).

Water carries ions through and around rocks. The effects of dissolved carbon dioxide and hydrogen ions and molecules can mix in solution to form a great variety of basic and acidic compounds. This is called solution. Solution tends to be the most effective in areas that have humid and hot climates (Pidwirny, 2006).

## **2.2. Physical Weathering**

Weathering or breakdown of stones by entirely mechanical processes is called physical weathering. Some of these processes originate within the stone, and some of them originate externally. The most important processes are abrasion, frost/thaw cycle, crystallization, thermal shock, wetting and drying and pressure release (Pidwirny, 2006).

**Abrasion:** When rock surfaces come together the friction or collision between the surfaces causes mechanical weathering or grinding of their surfaces which is called abrasion. Collision normally occurs during the erosion (transport of material by wind, water or ice) (Pidwirny, 2006).

**Frost/Thaw Cycle:** In temperate to cold climates, after seasonal freezing–thawing cycles, natural stone weathering occurs due to water stored in the pores and cracks of stone material. Frost damage has long been known as a major cause for deterioration. Frozen water causes pressure inside the material because the volume of water expands up to 9% when it freezes.

The pressure due to water expansion gives birth to new micro fractures, and present ones deepen and widen. After thawing, water can migrate into the newly developed

micro fractures. Recurrent freeze/thaw cycles cause enlarging of the existing fractures and further weakening of the material (Chen et al., 2004).

**Thermal Shock:** Sudden temperature changes without the presence of water also cause deterioration. Mineral components and of the interior and exterior portions of a stone show different expansion and contraction properties. Anisotropic thermal expansion can occur both within and between individual grains of such a sample. These processes lead to cumulative fatigue and formation of internal stresses, which can combine to generate tensile strain sufficient for micro fracturing to occur (Hale and Shakoor, 2003).

The rocks are not very good heat conductors. This inability to conduct heat results in different rates of expansion and contraction. The surface of the rock may expand more than its interior, and this stress eventually causes the rock to break down. The difference of colors of mineral grains in the rock may also cause differential expansion and contraction. Dark colored grains absorb more heat, and expand more than light colored grains. In a rock formed from with many different colored grains, expansion and contraction can occur at different rates at the various mineral boundaries (Pidwirny, 2006).

**Salt Crystallization:** Like frost, salt crystallization can cause stress to stones resulting in rupturing of rocks and minerals. The crystallization of salt results in 1 to 5 percent expansion depending on the temperature of the mineral surface. Salt weatherings mostly occur in hot arid regions (Pidwirny, 2006).

**Wetting and Drying:** Continuous cycles of wetting and drying of rocks is a very important factor in rock weathering. Water molecules accumulate as layers in between the mineral grains in the rock. This mechanism is called “ordered water”. The thickness of the layers increase gradually and this pulls the mineral grains with great tensional stress. Recent research has shown that slaking in combination with dissolved sodium sulfate can disintegrate samples of rock in only twenty cycles of wetting and drying (Pidwirny, 2006).

**Pressure Release:** The igneous rocks were formed deep under the Earth's surface at much higher pressures and temperatures. As these rock formations are brought to the surface by erosion, the pressure is released gradually. This unloading of pressure causes the rocks to fracture horizontally with an increasing number of fractures as the rock approaches the Earth's surface. Spalling, the vertical development of fractures, occurs because of the bending stresses of unloaded sheets across a three dimensional plane (Pidwirny, 2006).

### **2.3. Biological Weathering**

Biological weathering or “biodeterioration” of materials in nature cannot be considered as an isolated phenomenon. Biological factors may disintegrate rocks and minerals due to the chemical and physical agents released or applied by organisms (Caneva et al., 1991). Depending on the nature of the stone, the climatic conditions and the degree of pollution, different types of organisms may be seen on the stone surface. (Richardson et al., 1975). The types of organisms found mainly on stones are lichens, algae, fungi, moss and bacteria. Also plant and animal activities have some effect on stone deterioration.

Biological weathering can be either chemical or physical in character. Weathered stones may break down because of animal burrowing or by the pressure put forth by growing roots (Pidwirny, 2006).

Simple chemical processes like solution may be resulted by the carbon dioxide which is the product of respiration. Carbonic acid forms when carbon dioxide mix with water (Pidwirny, 2006).

Chelation is another process of biological weathering. It results in complex chemical reactions. Organisms produce organic substances called “chelates” that decompose minerals and rocks by removing metallic cations (Pidwirny, 2006).

Organisms can have effects on the moisture regime in soils. Usually, moisture increase in the environment is caused by the shade from leaves, the presence of roots masses, and humus. Since water is the most critical component in weathering processes, the contribution of organisms to the moisture is significant (Pidwirny, 2006).

Organisms can change the pH of the soil solution. Respiration from plant roots also releases carbon dioxide. The carbon dioxide mixes with water, carbonic acid is formed which makes soil more acidic. Again, when plants absorb nutrients from the soil, pH changes. The absorption processes often releases hydrogen ions. Generally, higher concentration of hydrogen ions makes the soil more acidic (Pidwirny, 2006).

## CHAPTER 3

### MATERIALS AND METHODS

In order to understand the deterioration processes, various archaeometrical methods such as petrography, X-ray powder diffraction analyses, analyses for determining basic physical properties (density, porosity, and water absorption capacities), ultrasonic velocity measurements and some mechanical tests are used. This chapter includes information about sample collection, definition of samples and methodology of the experiments carried on these samples. Results of the experiments are given in Chapter 4.

#### 3.1. Description of Samples

A total of five stone samples were collected from the site. The stones were collected from the foundation of the southern and eastern walls. Each sample was broken from the rocks the castle is built from. The samples include both the deteriorated surfaces facing outside and interior surfaces. They show similar deterioration characteristics with the walls of the castle.

The samples for the analyses and tests are prepared from these five stone pieces. The general visual characteristics of these stones may be summarized as follows:

**Stones 1 &3:** These are the least deteriorated samples. The surfaces of the stones are dirty but not flaked. Interior parts are fresh looking and unaltered.

**Stone 2:** This stone sample has a lichen covered surface and the surface is flaked. Interior parts are unaltered. (Figure 8)

**Stone 4:** This stone has a heavily deteriorated and flaked surface but the surface is relatively clean.

**Stone 5:** This is the most deteriorated stone that was collected from the foundation of the castle. Its interior parts are heavily deteriorated. (Figure 9)

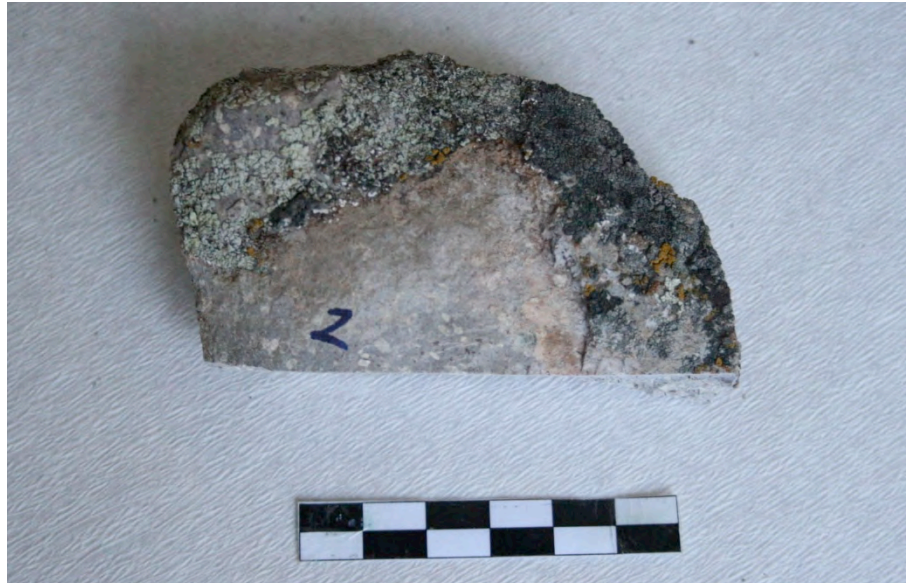


**Figure 8** Lichen covered and deteriorated surface of Stone 2



**Figure 9** Cut surface of Stone 5



### **3.2. Thin Section Analyses**

In order to determine the mineralogical and petrographical properties of the samples, one thin section from each sample was prepared in MTA laboratories. Then, the sections are analyzed under polarizing optical microscope (Leica DM4500 P) and they are photographed. The sections are also observed in order to determine the signs of and reasons for deterioration.

### **3.3. X-Ray Powder Diffraction Analyses**

All of the samples were examined by XRD method to determine the mineral composition and probable clay minerals, which may be responsible for deterioration.

#### **3.3.1. Unoriented XRD Sample Preparation and Methodology**

From each piece of rock generally more than one XRD sample were prepared. To be able to compare the mineralogical composition, samples were prepared both from the insides and the outsides of the stones. The properties of the stone samples are summarized in Table 1.

Since the stones contained very small amount of quartz phenocrystals, and it was not possible to distinguish the quartz in the ground mass, one sample is prepared from the ground mass of the Stone 1 to determine if there is quartz in the composition of the ground mass.

The most deteriorated stone, Stone 5 was collected from the foundation of the castle. Since this stone was heavily deteriorated, it was not possible to extract enough amount of fresh sample from this stone. The interior parts were also deteriorated.

**Table 1** Summary of the properties of samples prepared from each stone

Stone No	Sample No		
	Sample 1	Sample 2	Sample 3
<b>Stone 1</b>	Fresh sample from interior	Deteriorated sample from surface	Fresh sample from ground mass
<b>Stone 2</b>	Fresh sample from interior	Deteriorated flaked sample from surface	
<b>Stone 3</b>	Fresh sample from interior		
<b>Stone 4</b>	Fresh sample from interior	Deteriorated flaked sample from surface	
<b>Stone 5</b>	Deteriorated sample from interior	Deteriorated sample scraped from surface	

The samples were prepared according to the following procedure that was adopted from Carroll (1970):

To prepare the samples from the insides of the stones, pieces of about 50 grams were cut from each sample. After breaking the pieces into small pieces by the help of a hammer, they were pestled in an agate mortar. The powders were sieved and those passing # 200 mesh were selected. The powders from each sample were X-rayed to get unoriented mount for XRD analyses.

### **3.3.2. Oriented XRD Sample Preparation and Methodology**

The oriented X-ray powder diffraction analyses were made on five samples prepared from four different stones. These were Stone 1, Stone 2, Stone 4 and Stone 5.

Two samples were prepared from powdered samples from Stone 1, which is the freshest looking sample. But the surface looks dirty. To be able to compare the

interior and the near surface parts, one of the samples was prepared from the 5 cm interior of the stone. The other sample was prepared from the pieces broken from the 0-5 mm of the surface.

The sample from Stone 2 was prepared from flaked and lichen covered pieces on the surface. Lichen cover was removed gently from the surfaces of the pieces.



**Figure 10** Deteriorated and flaked surface of Stone 4

Stone 4 had a heavily flaked surface (Figure 10). But the air-dried clayey sample prepared from these flaked pieces did not show significant peaks. This was an expected result, because very little amount of clay was collected from this sample. The last sample was prepared from the dirtiest and the most deteriorated stone (Stone 5) by scraping a thin layer from the surface assuming that the clay minerals are concentrated near the surface (Figure 11).

After preparing the powder samples, clayey suspensions were prepared from each sample as described by Carroll (1970). After removing most of the water from the suspensions, the remaining clayey pastes were spread on cover slips and they were

air-dried. The clayey minerals formed thin layers on slips. The air-dried XRD analyses were made by placing the slips on the holder of the X-ray diffractometer.

After air-dried XRD analyses, air dried samples were ethylene glycolated and X-rayed. Then, the samples were placed in an oven set to 300°C for about one hour. The heated samples are X-rayed to get the heated, oriented XRD results (Carrol, 1970).



**Figure 11** Deteriorated and flaked surface of Stone 5

Brokner D8 Advance Diffractometer, Sol X detector was used for XRD analyses. Analyses were done using CuK radiation and the instrument was adjusted to 40 kV and 40 mA. For both the unoriented and oriented samples, the XRD traces were recorded for  $2\theta$  values.

### **3.4. Basic Physical Properties**

The physical properties of the stones were studied by the measurements of bulk density and total porosity using RILEM standard test methods (RILEM, 1980). In order to determine the physical properties of the samples collected from the site their porosity and ultrasonic pulse velocities are measured.

To find the bulk densities and porosities of the samples, their dry, wet and archimedes weights were measured.

The measurements were carried out with three different pieces from each stone. Two of the pieces were cut by taking into consideration that the deteriorated surface of the sample is included. And one piece was cut from the inside of the sample. The purpose of this procedure is to determine whether there is any difference between the surface and the inside of the stones.

To obtain the wet weights, the samples were left in distilled water for 24 hours. Then, in order to remove the remaining air inside the pores vacuum was applied (with pressure about 100 mmHg) for half an hour and then vacuum was released, samples were left in water for one hour. This process was repeated two times in order to saturate the samples.

After wiping the water droplets, the samples were weighed. This was repeated three times for each sample in order to minimize the error in the measurements.

To measure the Archimedes weights of the pieces, each water-saturated piece was immersed into water and then their weights were measured. This procedure and measurements were also repeated three times to minimize the error.

In order to obtain the dry weights of the pieces, the pieces were air dried in an oven set to 60°C for 24 hours. Then, they were weighed.

### 3.4.1. Porosity

Effective porosity (P) is defined as the percentage of the total volume of a porous material occupied by pores or more simply the empty spaces or voids in the mass. It is formulated as follows (RILEM 1980):

$$P (\% \text{ volume}) = 100 \times (m_{\text{sat}} - m_{\text{dry}}) / (m_{\text{sat}} - m_{\text{arch}})$$

where:  $m_{\text{sat}}$ : water saturated weight (g)

$m_{\text{dry}}$ : dry weight (g)

$m_{\text{arch}}$ : Archimedes weight (weight of the sample in water) (g)

### 3.4.2. Bulk Density

Bulk density (D) is the ratio of the mass to the bulk volume of the sample and is formulated as follows (RILEM 1980):

$$D (\text{g/cm}^3) = m_{\text{dry}} / (m_{\text{sat}} - m_{\text{arch}})$$

where:  $m_{\text{sat}}$ : saturated weight (g)

$m_{\text{dry}}$ : dry weight (g)

$m_{\text{arch}}$ : archimedes weight (weight of the sample in water) (g)

### 3.4.3. Water Absorption Capacity

Water absorption capacity (WAC) is the amount of water that the material can absorb. The water absorption capacity is the difference between water saturated mass and Archimedes weight divided by Archimedes weight. The formula is (RILEM 1980):

$$\text{WAC} (\% \text{ weight}) = 100 \times (m_{\text{sat}} - m_{\text{dry}}) / m_{\text{dry}}$$

where:  $m_{\text{sat}}$ : saturated weight (g)

$m_{\text{dry}}$ : dry weight (g)

### 3.5. Ultrasonic Pulse Velocity Measurements

In order to understand the physical properties of the stones, ultrasonic pulse velocities in the collected samples were measured. The transmission time of the ultrasonic pulses in the stones were measured by a pulse generating test equipment, PUNDIT plus. The distances between the probes were also measured with the help of a caliper.

The ultrasonic pulse velocities are calculated by using the following formula (RILEM, 1980):

$$V = l / t$$

where: V: ultrasonic velocity (mm/s)

l: the distance traveled by the wave (cross section of specimen) (mm)

t: travel time (s)

To observe the transmission of ultrasonic waves inside the stones, three different methods are used:

#### **Direct measurements**

Direct measurements involve taking measurements of pulse transmission times of ultrasonic waves passing through the samples. The probes are located at opposite surfaces of the samples facing each other. Direct transmission is defined as the propagation of ultrasonic stress waves along a straight-line path between the opposite surfaces of a specimen. (Yaman et al, 2001)

The measurements were taken from different parts of the samples. Since the samples are of different shape and size, the number of measured parts was not the same. But for each part at least three different measurements were taken in order to minimize the error.

### **Indirect measurements**

Indirect measurements involve taking measurements of pulse transmission times of ultrasonic waves transmitting from near the surface. The probes are positioned at the same surface of the specimen.

Many studies have been conducted on direct pulse velocity determination and factors that affect it. Standards are available for measuring velocity using direct transmission. Less information is available on indirect transmission. Generally, indirect transmission is used when only one surface of the material structure is accessible. It is often stated that indirect measurements are not reliable (Yaman et al, 2001).

In this study, indirect measurements from the deteriorated and fresh surfaces gave an opportunity to compare the physical status of the surfaces. It is assumed that the comparison of transmission times at the deteriorated and the fresh surfaces may give idea about the degree of deterioration near the surface. The measurements were taken from the outer deteriorated surfaces and cut interior surfaces.

### **Indirect measurements with one probe fixed**

Indirect measurements with one probe fixed involve taking measurements of pulse transmission times of ultrasonic waves transmitting from near the surface. These measurements were taken from the exterior, weathered surfaces of the stones. With one probe fixed, the distance between the probes was changed by moving the other probe linearly and transmission times were recorded. The measurements were carried out on three samples (Stone 1, Stone 2, and Stone 3). Stone 1 was chosen as a minimum deteriorated sample and Stones 4 & 5 were chosen as the most deteriorated samples. The aim of these measurements was to determine relationship between the ultrasonic velocity and the probe distance at the deteriorated surfaces.



### 3.6. Modulus of Elasticity

One of the important material properties is expressed by the modulus of elasticity ( $E_{mod}$ ) value, which could be indirectly obtained from ultrasonic pulse velocity measurements. Modulus of elasticity is the mathematical description of an object or substance's tendency to be deformed elastically when a force is applied to it.

The modulus of elasticity is then obtained through the bulk density of the specimen and ultrasonic velocity by the following formula (RILEM, 1980):

$$E_{mod} = D \times V^2 (1 + \gamma_{dyn})(1 - 2\gamma_{dyn}) / (1 - \gamma_{dyn})$$

Where:  $E_{mod}$ : modulus of elasticity ( $N/m^2$ )

D: bulk density of the sample ( $kg/m^3$ )

V: velocity of wave (m/sec)

$\gamma_{dyn}$ : Poisson's Ratio\*

\*Poisson's ratio (ratio of transverse contraction strain to longitudinal extension strain in the direction of stretching force) is taken as 0.19 in these measurements. (Özsan, 2006)

### 3.7. Durability Tests

These tests were made during a previous study on the building stones of the Kalecik Castle. These tests were carried out by a group led by Prof. Dr. Tamer Topal of Geological Engineering Department, METU. These physico-mechanical tests consist of frost/thaw and salt crystallation cycles.

Freezing-thawing test simulates the effects of ice crystals formed within the pores of the stone below 0°C. It is recommended if water absorption under atmospheric conditions is more than 1%. In this study, the cubic samples are submerged in water for 24 hours and then they are put into deep-freeze cabinet (RILEM, 1980). The

temperature of the cabinet varies between  $-15^{\circ}\text{C}$  and  $+2^{\circ}\text{C}$  within a period of 12 hours.

Salt crystallization tests may include two types of salt. They are magnesium sulphate ( $\text{MgSO}_4$ ) and sodium sulphate ( $\text{Na}_2\text{SO}_4$ ). However, the sodium sulphate is very frequently used to understand the stone deterioration, and therefore it is used following RILEM (1980) in this study. Density, porosity, water absorption capacity, sonic velocity, and unconfined compressive strength of the dacitic rocks through cycles were calculated.

## CHAPTER 4

### EXPERIMENTAL RESULTS

This chapter includes the results of experiments and observations consisting of thin section analyses, X-ray powder diffraction analyses, analyses for determination of basic physical properties (density, porosity, and water absorption capacities), ultrasonic pulse velocity measurements and mechanical tests. The methodologies of the tests are described in Chapter 3.

#### 4.1. Thin Section Analyses

According to the thin section analyses, the stones collected from the castle consist of mainly plagioclase. This is a group of feldspar minerals that have the same formula, but vary in their percentage of sodium and calcium. The series include Albite, Anorthite, Oligoclase, Andesine, Labradorite and Bytownite (Streckeisen, 1974). The plagioclase feldspars occur in many mineral environments. It is very hard to tell apart one from another. In case plagioclase feldspar cannot be identified, it is simply called "plagioclase" or "plagioclase feldspar". There are also hornblende phenocrystals in the castle rock. There is very little number of biotite phenocrystals.

During the thin section analyses, on the Kalecik Castle stone specimens, multiple crystal twinning is observed. This occurs when two separate crystals share some of the same crystal lattice points in a symmetrical manner. If several twin crystal parts are aligned by the same twin law they are referred to as multiple or repeated twins.

Dacite consists mostly of plagioclase feldspar with biotite, hornblende, and pyroxene (augite and/or enstatite). It has quartz as rounded, corroded phenocrysts, or as an element of the ground-mass. According to the QAPF diagram dacite may have a quartz ratio between 20% and 60% (Streckeisen, 1974).

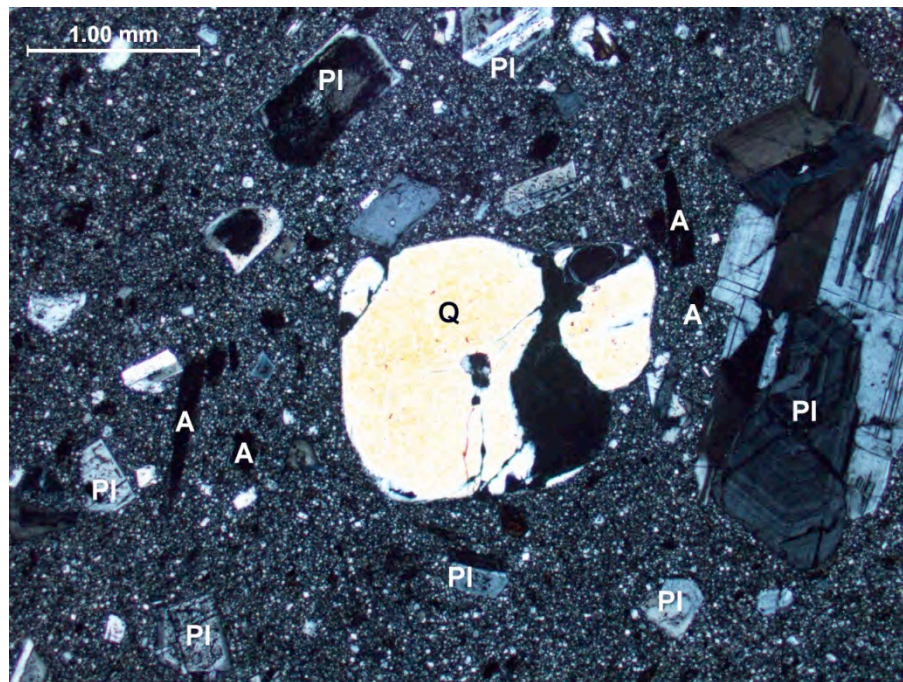


**Figure 12** Thin section photograph from Stone 1 showing a large quartz phenocrystal and a large glomeroporphyritic plagioclase phenocrystal (Pl: Plagioclase, Q: Quartz, A: Amphibole)

Minerals are glomeroporphyritic or cumulo-phyrritic, which refers to the grouping of phenocrysts, not necessarily of the same mineral, into distinct clusters within porphyritic igneous rocks (Figure 12).

The rock has a porphyritic and aphanitic structure. There are distinct differences in the sizes of the crystals. Ground mass contains very fine grained crystals whose components are not detectable by naked eye. In addition especially in sample 1, the crystals forming the ground mass is hard to define under the microscope because they are too small. Supported by XRD analyses, we can conclude that these very

fine-grained minerals are probably plagioclase feldspar, hornblende, quartz and also smaller amounts of biotite. There are some quartz phenocrysts, which has diameters up to 2 millimeters (Figure 12).



**Figure 13** A large plagioclase phenocrystal having sieve texture

Some plagioclase crystals have sieve texture (also called moth-eaten texture) and they are also very lightly clayey plagioclase (Figure 13). There are also smaller phenocrysts which are opaque. There are opaque mafic minerals (rich in magnesium and iron). Amphibole is partially or completely altered to opaque.

The groundmass has a felsitic texture. It is composed of plagioclase in the form of microlith and micrograins, very small grains of quartz and also opaque minerals in the form of micrograins. This definition based on the optical observations is supported by X-ray diffraction analyses.

Ground mass shows sericitization (the hydrothermal or metamorphic replacement of a mineral, often plagioclase, by sericite (white mica)) from place to place but very small amounts of this replacement was observed here.

During the petrologic investigation some fractures and micro faults are also observed. Some of the fractures cross minerals and the minerals show angular deformations. Therefore, we can conclude that these fractures are the remains of the solidification process of the rock. In other words, these fractures are probably not the results of weathering processes.

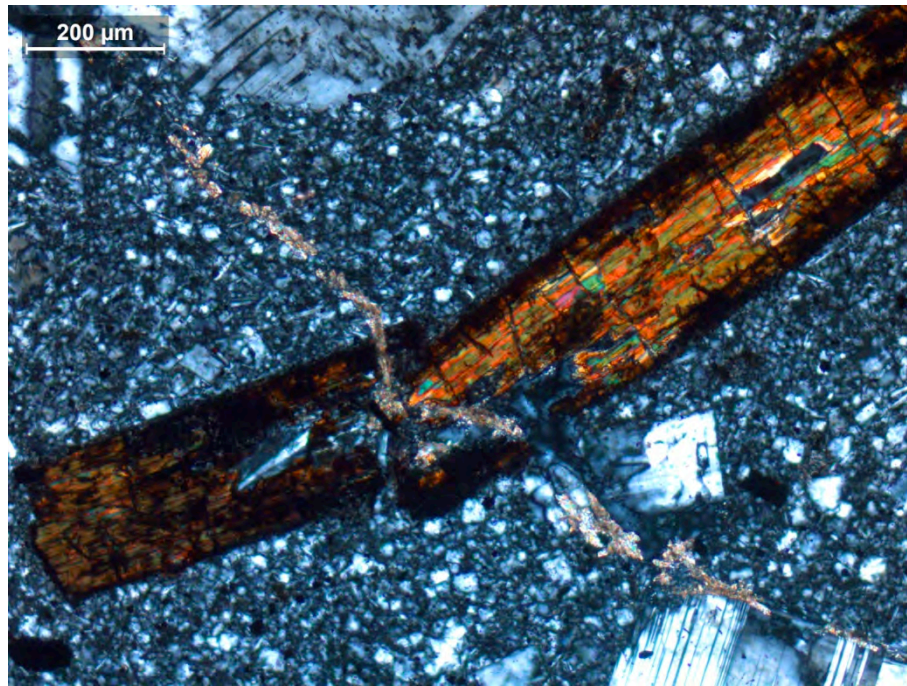


**Figure 14** Carbonate filling in one of the fractures in Stone 5

In terms of mineral composition, all of the samples show the similar characteristics. The most important difference is that one of the five stone samples (Stone 5) has more fractured structure and the fractures are partially filled with carbonate (Figure 14). Sample 5 is the most deteriorated sample which was collected from the base of the castle.

Excluding fractures and carbonate fill, there are only slight differences seen between the samples.

## 4.2. X-Ray Powder Diffraction Analyses

The X-ray powder diffraction analyses show that the building stones have typical mineral composition of dacitic rocks supporting the petrographical analyses. In unoriented X-ray powder diffraction analyses, strong lines of quartz and plagioclase group of feldspars are easily distinguishable (Figure 15). All of the samples have similar plots.

The oriented X-ray powder diffraction analyses showed that all of the samples contain smectite group clay minerals. In air-dried samples a peak in the range 12 Å to 15 Å is present which expands uniformly to 17.2 Å after ethylene glycolation.

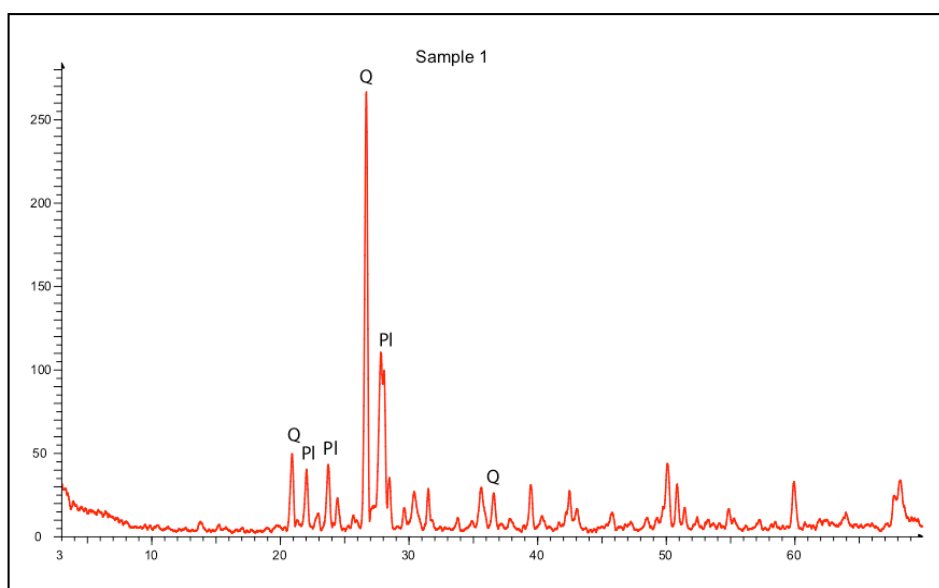


**Figure 15** X-ray powder diffraction plot of powder sample prepared from Stone 1.  
(Q: Quartz, P: Plagioclase)

The most deteriorated sample (collected from Stone 5) also contains Illite and Kaoline group of clay minerals.

X-ray powder diffraction charts are given in Appendix.

### 4.3. Basic Physical Properties

The results of the calculations regarding the basic physical properties of the stone samples are given in tables and graphs. In graphs, the results from the fresh and the deteriorated samples are expressed in collateral lines for comparison.

#### 4.3.1. Porosities

The porosity test results on the samples are given in Table 2 and plotted on Figure 16. The porosity values vary from 8.30% to 13.33%. Based on the results, it may be stated that except Sample 1, deteriorated samples have higher porosities. This is attributed to the effect of deterioration.

**Table 2** Calculated porosities of samples

Deteriorated Samples		Fresh Samples	
Sample	P (% Vol)	Sample	P (% Vol)
1	11.40	1	11.91
2	12.37	2	8.30
3	10.89	3	8.65
4	13.33	4	10.72
5	11.20	5	11.12

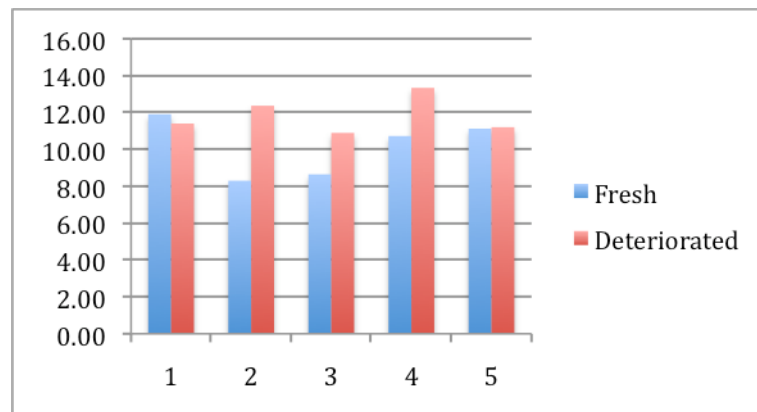


**Figure 16** Porosity comparison of each sample's fresh and deteriorated parts



### 4.3.2. Bulk Densities

The bulk density test results on the samples are given in Table 3 and plotted on Figure 17. The bulk density values are generally in the range of 2.28-2.37 g/cm<sup>3</sup>. Based on the results, it may be stated that very slight changes are observed for the samples. Therefore, this is not a good parameter for the assessment of state of deterioration.

**Table 3** Calculated bulk densities of samples

Deteriorated Samples		Fresh Samples	
Sample	D (g/cm <sup>3</sup> )	Sample	D (g/cm <sup>3</sup> )
1	2.30	1	2.28
2	2.26	2	2.37
3	2.32	3	2.35
4	2.31	4	2.36
5	2.35	5	2.37

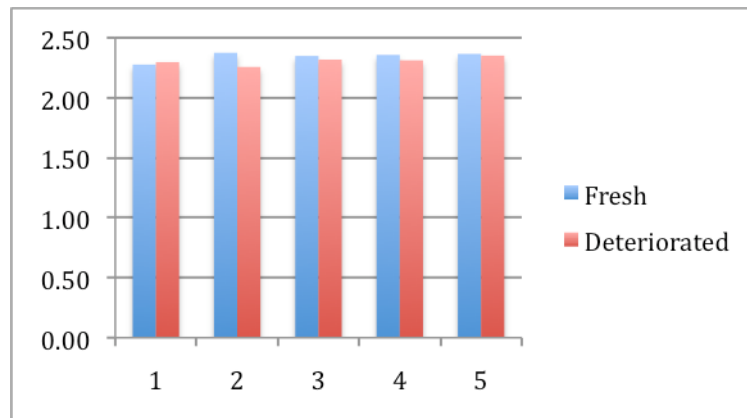


**Figure 17** Bulk density comparison of each sample's fresh and deteriorated parts

### 4.3.3. Water Absorption Capacities

The water absorption test results on the samples are given in Table 4 and plotted on Figure 18. The absorption values range between 3.68% and 5.77%. Based on the results, it may be stated that except Sample 1, deteriorated samples have higher water absorption values. This is attributed to the effect of deterioration.

**Table 4** Calculated water absorption capacities of samples

Deteriorated Samples		Fresh Samples	
Sample	WAC (%)	Sample	WAC (%)
1	4.96	1	5.23
2	5.49	2	3.50
3	4.70	3	3.68
4	5.77	4	4.55
5	4.77	5	4.70

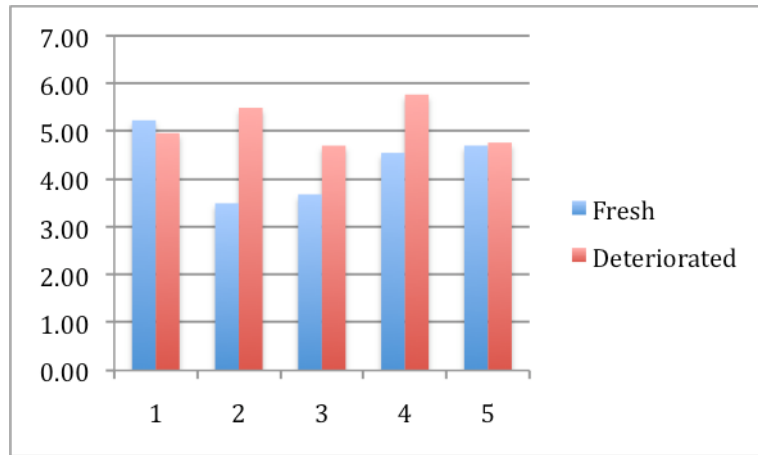


**Figure 18** Water absorption capacity comparison of each sample's fresh and deteriorated parts

#### 4.4. Ultrasonic Pulse Velocity Measurements

##### 4.4.1. Direct Measurements

Direct measurements involve taking measurements of pulse transmission times of ultrasonic waves passing through the samples. The calculated values of ultrasonic pulse velocity for each sample are given in Table 5 and plotted in Figure 19. The values range between 556.36 m/s and 3065.48 m/s indicate significantly different state of weathering. Lower sonic velocity in Sample 5 clearly indicates that it is highly deteriorated.

**Table 5** Ultrasonic pulse velocities of the samples (direct measurement)

Sample	Ultrasonic Velocity (m/s)
1	1785.21
2	1439.08
3	3065.48
4	1376.04
5	556.36

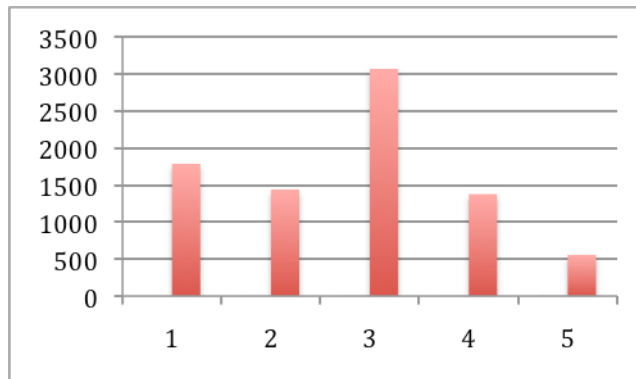


**Figure 19** Ultrasonic pulse velocities in samples (direct measurement)

#### 4.4.2. Indirect Measurements from Surface (Exterior)

Indirect measurements involve taking measurements of pulse transmission times of ultrasonic waves transmitting from near the exterior surface. The probes are positioned at the same surface of the specimen. The calculated values of ultrasonic pulse velocity for each sample are in Table 6 and plotted in Figure 20. Lower values reveal deteriorated nature of the samples.

**Table 6** Ultrasonic pulse velocities of the samples (indirect measurement from the surface)

Sample	Ultrasonic Velocity (m/s)
1	1629.50
2	2009.30
3	2389.02
4	no measurement
5	no measurement

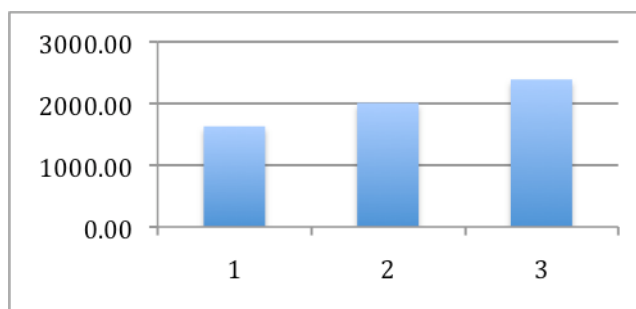


**Figure 20** Ultrasonic pulse velocities in samples (indirect measurement)

#### 4.4.3. Indirect Measurements from Surface (Interior)

Indirect measurements involve taking measurements of pulse transmission times of ultrasonic waves transmitting from near the cut surface (interior). The probes are positioned at the same surface of the specimen. The calculated values of ultrasonic pulse velocity for each sample are given in Table 7 and plotted in Figure 21. Lower values again indicate stone deterioration.

**Table 7** Ultrasonic pulse velocities in samples (indirect measurement from the inside)

Sample	Ultrasonic Velocity (m/s)
1	2135.64
2	2072.53
3	2454.72
4	no measurement
5	no measurement

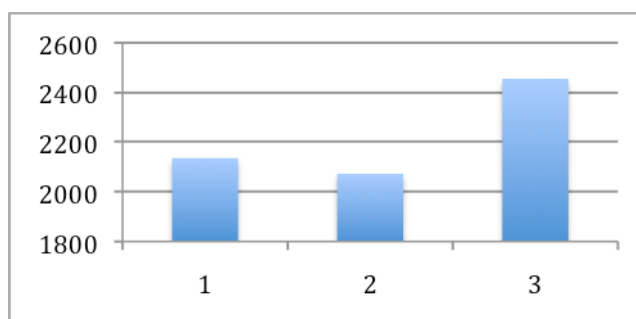


**Figure 21** Ultrasonic pulse velocities in samples (indirect measurement from the inside)

#### 4.4.4. Indirect Measurements with one Probe Fixed

These measurements were taken from the exterior, weathered surfaces of the stones. With one probe fixed, the distance between the probes was changed by moving the other probe linearly and transmission times were recorded. These measurements (Tables 8-10 and Figures 22-24) were carried out on three samples (Stone 1, Stone 2, Stone 3). Lower values indicate deteriorated stones.

#### Stone 1

**Table 8** Indirect ultrasonic velocity measurements with one probe fixed for Stone 1

Probe Dist. (cm)	UV (m/s)
3.74	1795.20
5.49	1149.34
6.85	1524.48
8.00	1674.81

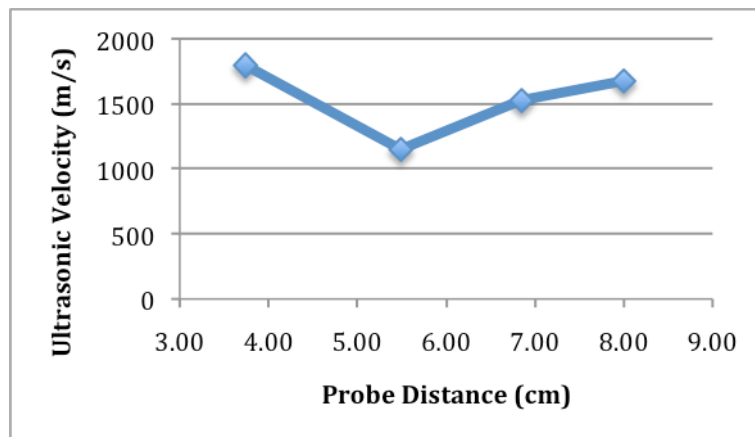


**Figure 22** Indirect ultrasonic velocity measurements with one probe fixed for Stone 1

## Stone 4

**Table 9** Indirect ultrasonic velocity measurements with one probe fixed for Stone 4

Probe Dist. (cm)	UV (m/s)
3.74	1795.20
5.49	1149.34
6.85	1524.48
8.00	1674.81

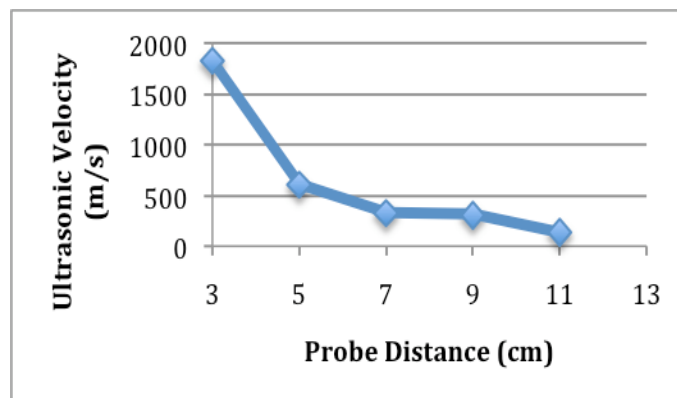


**Figure 23** Indirect ultrasonic velocity measurements with one probe fixed for Stone 4

## Stone 5

**Table 10** Indirect ultrasonic velocity measurements with one probe fixed for Stone 5

Probe Dist. (cm)	UV (m/s)
3	1487.60
6	1170.35
9	1053.86
12	339.30

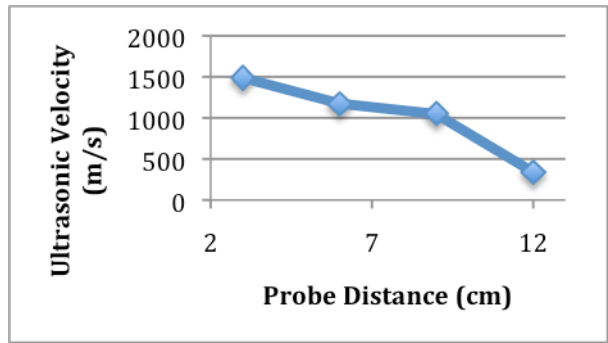


**Figure 24** Indirect ultrasonic velocity measurements with one probe fixed for Stone 5

#### 4.5. Modulus of Elasticity

The moduli of elasticity of the samples are calculated by using the data from ultrasonic pulse velocities. The calculated values are given in Table 11 and the variations of the values are shown in Figure 25. Lower modulus of elasticity values show deteriorated state of the rocks.

**Table 11** Modulus of elasticity calculations for stone samples

Sample	$E_{mod}$ (N/m <sup>2</sup> )
1	6539.67
2	4417.34
3	19875.07
4	4021.78
5	660.25

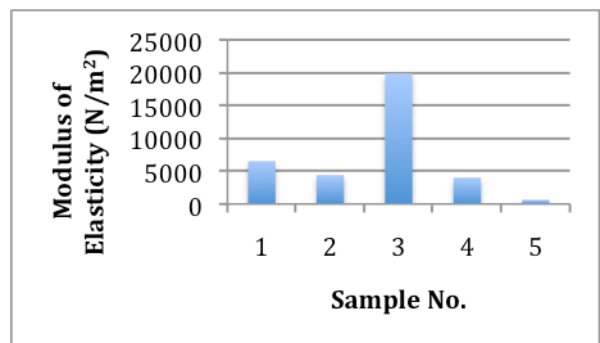


**Figure 25** Modulus of elasticity calculations for stone samples

#### 4.6. Durability Tests

For the durability tests, freeze/thaw and salt crystallization tests are conducted following RILEM (1980). At various test cycles (10, 20, 30, 45, 55) dry and saturated unit weights, porosity, water absorption, uniaxial compressive strength and sonic velocity tests are performed. The test results and presented in Tables 12, 13 and 14, and the variation of the physico-mechanical properties of the samples are shown in Figures 26-33. The test results indicate that except unit weight, all the other properties yield useful information about state of stone deterioration since they change with test cycles.

**Table 12** Changes in samples after repeated freeze/thaw cycles

Number of Cycle	Dry Unit Weight (gr.)	Saturated Unit Weight (gr.)	Dry Density (gr/cm <sup>3</sup> )	Saturated Density (gr/cm <sup>3</sup> )	Porosity (%)	Water Absorption	U.C.S. (MPa)	Sonic Velocity (m/sec)
0	23.16	24.08	2.36	2.45	9.35	0.04	66.17	3402.12
10	23.22	24.13	2.37	2.46	9.10	0.04	60.94	3508.58
20	23.30	24.25	2.38	2.47	9.32	0.04	61.25	3294.13
30	23.08	24.16	2.35	2.46	9.74	0.04	58.53	2622.76
45	23.51	23.72	2.40	2.42	11.07	0.05	49.83	2225.58
55	23.16	24.06	2.36	2.45	12.39	0.05	32.61	1534.38

**Table 13** Changes in samples after repeated salt crystallization cycles

Number of Cycle	Dry Unit Weight (gr.)	Saturated Unit Weight (gr.)	Dry Density (gr/cm <sup>3</sup> )	Saturated Density (gr/cm <sup>3</sup> )	Porosity (%)	Water Absorption	U.C.S. (MPa)	Sonic Velocity (m/sec)
0	22.25	23.13	2.27	2.36	8.97	0.04	66.17	3416.53
10	23.16	24.06	2.36	2.45	9.21	0.04	53.79	2657.61
20	23.15	24.22	2.36	2.47	10.99	0.05	51.95	2457.99
30	23.48	24.48	2.39	2.50	10.14	0.04	52.37	1979.30
45	18.72	19.65	1.91	2.00	13.10	0.05	30.69	1538.00
55	23.36	24.73	2.38	2.52	13.96	0.06	25.14	960.01



**Table 14** Changes in Unconfined Compressive Strength / Porosity Ratios after repeated cycles

Freeze-Thaw		Salt-Crystallization	
Number of Cycle	U.C.S / Porosity Ratio	Number of Cycle	U.C.S / Porosity Ratio
0	7.08	0	7.38
10	6.70	10	5.84
20	6.57	20	4.73
30	6.01	30	5.16
45	4.50	45	2.34
55	2.63	55	1.80

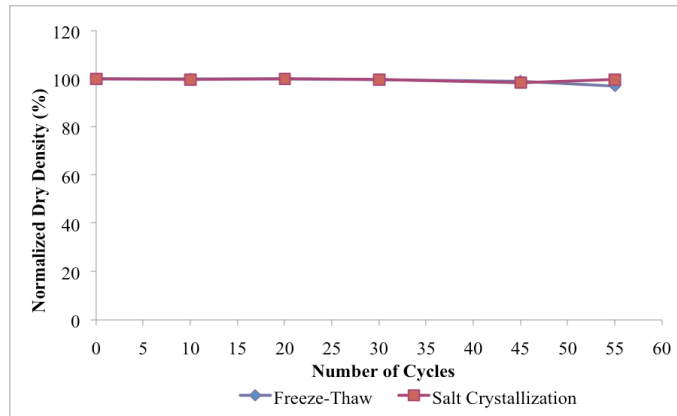


**Figure 26** Change in dry densities after repeated freeze/thaw and salt crystallization cycles

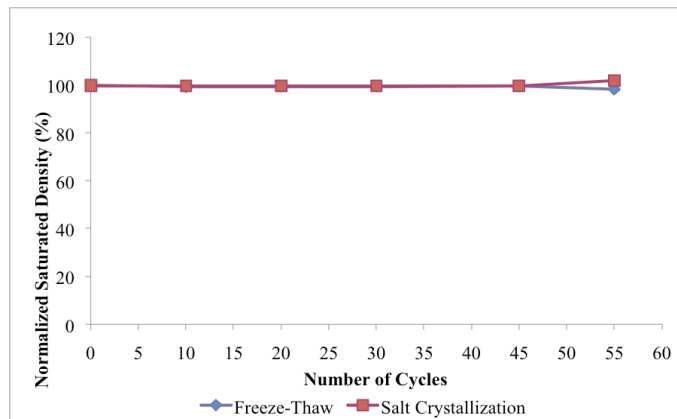


**Figure 27** Change in saturated densities after repeated freeze/thaw and salt crystallization cycles

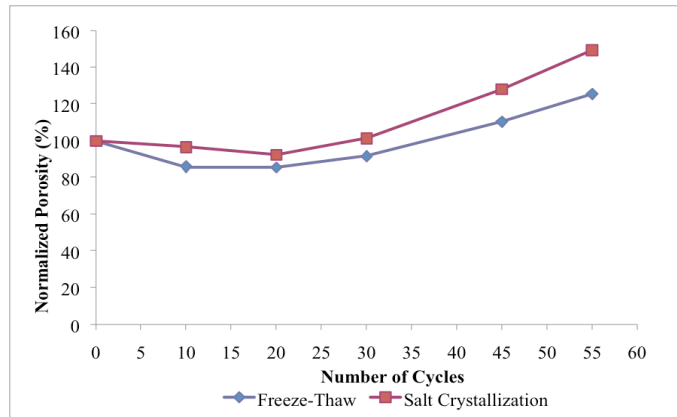


**Figure 28** Change in porosities after repeated freeze/thaw and salt crystallization cycles

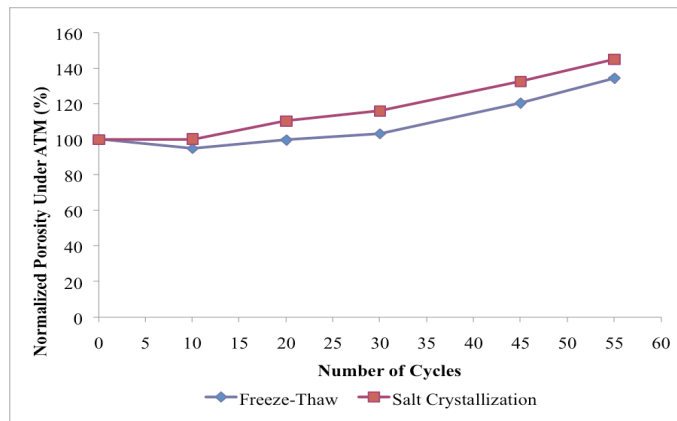


**Figure 29** Change in porosity after repeated freeze/thaw and salt crystallization cycles under atmospheric pressure

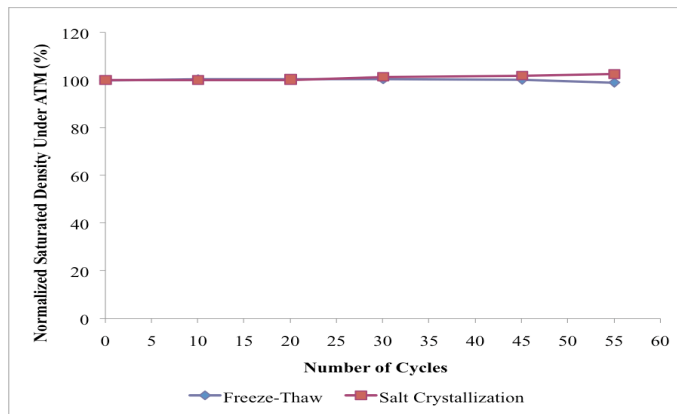


**Figure 30** Change in saturated densities after repeated freeze/thaw and salt crystallization cycles under atmospheric pressure

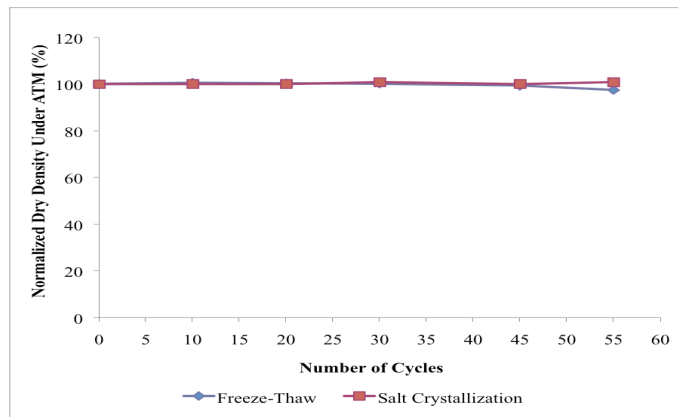


**Figure 31** Change in dry densities after repeated freeze/thaw and salt crystallization cycles under atmospheric pressure

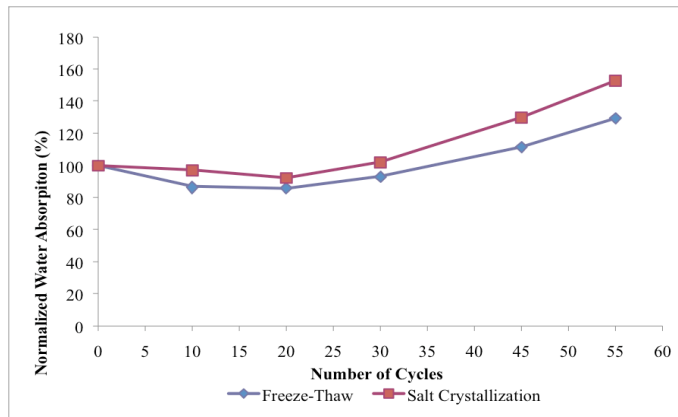


**Figure 32** Change in water absorption capacities after repeated freeze/thaw and salt crystallization cycles

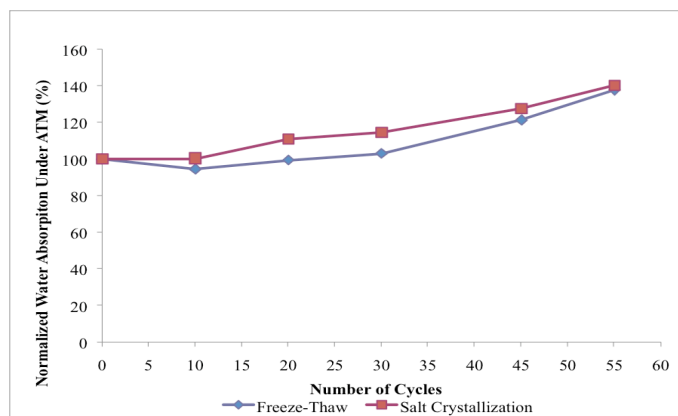


**Figure 33** Change in water absorption capacities after repeated freeze/thaw and salt crystallization cycles under atmospheric pressure

## CHAPTER 5

### CONCLUSIONS

In this study, the building stones of Kalecik Castle have been investigated in order to understand the deterioration mechanisms. The deterioration at the stones forming the walls and the rocks forming the base of the castle is visually detectable. The cracks, material loss and the color change are noticeable. In order to determine the mechanisms of deterioration, some arhaeometrical methods such as petrography, X-ray diffraction analyses, and analyses for determining the physico-mechanical properties are used. The data obtained from a previous study are also used to understand the material's deterioration behavior under repeated cycles of freeze/thaw and salt crystallation. The summary of discussions about the observations and the laboratory tests are as following:

The volcanic rocks in Kalecik region are named as Kalecik Volcanite and defined as “dacite” in the geological map of the region (Dönmez, 2010). These studies may be carried on mainly Gökdere region where the Kalecik Volcanite is more widespread. But, in this study the type of the building stone is also determined as dacite by petrographic analyses supported by X-ray diffraction analyses.

Petrographic studies, which involve the examination of thin sections prepared from the stone samples collected from the castle points out that the deterioration may be physical. The slight deterioration of minerals occurs during the formation of the rocks. Therefore the effects of chemical processes, which are important factors on rock weathering, may be eliminated.

Petrographic analyses show that there are some fractures and micro-scale faults in the stones. Some of these fractures cross minerals and the minerals show angular deformations. This means that these fractures are the remains of the solidification process of the rocks. In other words, these cracks are probably not the results of weathering processes, but the presence of these fractures might have brought up the physical processes that deteriorated the rocks.

Most of the fractures observed in thin sections are empty. The only sample, which has partially filled fractures, was collected from the base of the castle that probably had been in contact with soils. The material filling the fracture is carbonate. Since the carbonate filling is only observed in the sample which may have contacted with soil, it can be concluded that the empty fractures which crosses the minerals and reaches to surface of the cut stones have paved the way for water absorption.

The X-ray diffraction analyses show that the building stones have typical mineral composition of dacitic rocks supporting the petrographical analyses. According to the oriented X-ray diffraction analyses, all of the samples contain small amount of smectite group clay minerals. The most deteriorated sample, which was collected from the base of the castle, also contains illite and kaoline group of clay minerals, which is possibly resulted from soil contact. The detection of clay minerals is important because clay minerals swell in aqueous conditions. The repeated cycles of this swelling breaks down the rocks.

The physical tests carried on fresh and deteriorated parts of the stone samples show that porosity and water absorption capacities increase by deterioration. The physico-mechanicals tests support these results. After repeated cycles of freeze/thaw and salt crystallation tests, the porosities and water absorption capacities are also increased significantly.

According to the ultrasonic velocity tests, ultrasonic velocities decrease by increasing the probe distance in deteriorated samples. The more the sample is deteriorated, the more the ultrasonic velocities decrease by probe distance. This

indicates that the deteriorated stones have more spaces like porosities, fractures and cracks.

Visual observations in the field and in the laboratory show that biological deterioration might also have a role in deterioration, at least in some parts of the castle. There are some lichen formations especially at the base parts of the castle. But the stone surfaces where lichens are not found are almost as deteriorated as the lichen covered surfaces. The lichen-covered surface of stone sample brought to laboratory has similar petrographical and oriented X-ray diffraction characteristics with the cleaner parts of the sample.

The dacitic stone probably mined from the small volcanic cone where the castle is located is also used as building stone in many historical buildings in Kalecik. Visual examination of the building stones shows that they are also subject to similar kinds of deterioration. Material loss and flaking on the surface are clearly visible at outer walls that are especially open to weathering agents such as water, frost etc.

In conclusion, the deterioration of Kalecik Castle results mainly from physical and mechanical factors such as freeze/thaw and salt crystallization cycles, wetting-drying and thermal shock. Any sign of chemical factors has not been observed and biological factors are considered to be negligible. The natural porous and fractured structure of the building stone combined with the region's though climate where many freeze thaw cycles and sudden temperature differences occur, results in deterioration of the stones.

## REFERENCES

- Aslangil, H. C., Ekiz, H. H., *Kalecik'in Tarihi: Dünü Bugünü için Bir Araştırma*, Kalecik Kültür Derneği Yayını No: 1, 1996.
- Blatt, H., Tracy, R., *Petrology*, Freeman, ISBN 0-7167-2438-3, 1996.
- Böke, H. Akkurt, S., İpekoğlu, B., *Tarihi Yapılarda Kullanılan Horasan Harcı ve Sıvalarının Özellikleri*, Yapı, Nisan 2004.
- Carroll D. *Clay minerals: a guide to their X-ray identification: special paper 126*. Boulder, CO: The Geological Society of America. 80 p., 1970.
- Caneva, G., Nugari, P.M., Salvadori, O., *Biology in The Conservation of Works of Art*, ICCROM-International Centre for the Study of the Preservation and the Restoration of Cultural Property, Rome RM, Italy, 1991.
- Chen TC, Yeung MR, Mori N. *Effect of water saturation on deterioration of welded tuff due to freeze-thaw action*. Cold Regions Sci Technol 2004; 38:127–36.
- Dorsey, J., Edelman, A., Jensen, H.W., Legakis, J., Pedersen, H.K., *Modeling and Rendering of Weathered Stone*, SIGGRAPH conference proceedings, 1999.
- Dönmez, M., Akçay, A.E., Türkecan, A., Satır, M., Evcimen, Ö., Gündoğdu, E.A., Görmüş, T., *Ankara ve Yakın Çevresi Geç Kretase–Tersiyer Volkanitlerinin Stratigrafisi ve Yeni Yaş Bulguları*, 62. Türkiye Jeoloji Kurultayı, Bildiri Özleri Kitabı, Cilt 2, S.632, Ankara, 2009.
- Dönmez M., Akçay, A.E., *Türkiye Jeoloji Haritaları No: 138, Çankırı – H 30 Paftası*, Maden Tetkik ve Arama Genel Müdürlüğü, Ankara, 2010.
- Gill, R., *Igneous Rocks and Processes: A Practical Guide*, John Wiley & Sons, Oxford, 2010.
- Hale P.A., Shakoor A. *A laboratory investigation of the effects of cyclic heating and cooling, wetting and drying, and freezing and thawing on the compressive strength of selected sandstones*, Environ Eng Geosci 2003; 9:117–30.

- Özsan A., Başarır, H., Cılsal, M. *Engineering geological investigations along the Ankara subway extension*, The 10th IAEG Congress, Nottingham, United Kingdom, 6-10 September, 2006.
- Pidwirny, M. *"Weathering". Fundamentals of Physical Geography, 2nd Edition*, 2006. (<http://www.physicalgeography.net/fundamentals/10r.html>)  
(Last Access: 21/12/2011)
- Raftery, T., Clay Analysis by XRD, *Clay Analysis by XRD*, Australian X-ray Analysis Association Web Site ([www.axaa.org](http://www.axaa.org)) (Last Access: 09/12/2011).
- RILEM, *Recommended tests to measure the deterioration of stone and to assess the effectiveness of treatment methods*, Commission 25-PEM, Material and Structures, Vol.13, p.175-253, 1980.
- Sari, M., Karpuz, C., Anday, C., *Estimating rock mass properties using Monte Carlo simulation: Ankara andesites*, Computers & Geosciences, Volume 36, Issue 7, July 2010, Pages 959-969.
- Schaffer, R.J., *The Weathering of Natural Building Stones, Department of Scientific and Industrial Research*, Building Research Special Report No. 18, p.10-82., 1972.
- Streckeisen, A. L., *Classification and Nomenclature of Plutonic Rocks*, Recommendations of the IUGS Subcommission on the Systematics of Igneous Rocks. Geologische Rundschau. Internationale Zeitschrift für Geologie. Stuttgart. Vol.63, p. 773-785, 1974.
- Tokmak, M., *Documentation and Examination of Historic Building Materials for the Purpose of Conservation: Case Study, Part of the Walls at the Citadel of Ankara*, 2005.
- Yaman, O., İnci, G., Yeşiller, N., Aktan, H.M., *Ultrasonic Pulse Velocity in Concrete Using Direct and Indirect Transmission*, ACI Materials Journal, November/December 2001.



## APPENDIX

### X-RAY POWDER DIFFRACTION CHARTS

The samples are examined under XRD to determine the mineral composition and probable clay minerals that may be responsible for deterioration. From each piece of rock generally more than one XRD sample is prepared. To be able to compare the mineralogical composition difference between the interior and the exterior parts of the stone samples are prepared from the inside and from the surface. The samples contained powder from each sample's interior and near-surface flaked parts. These are described under each chart.

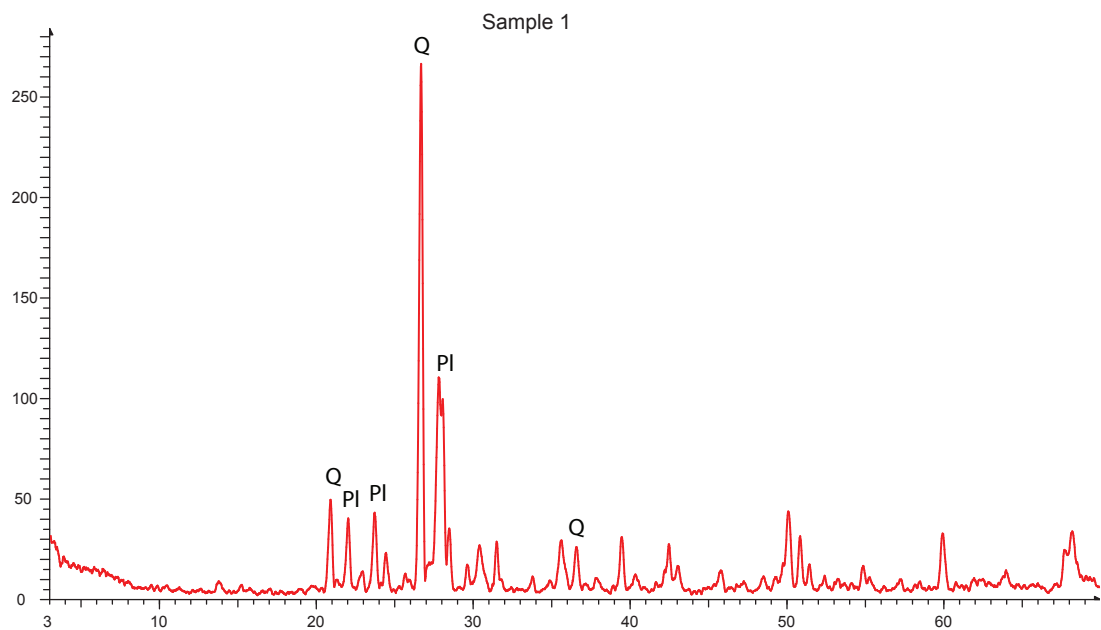


**Figure 34** X-ray diffraction chart for samples collected from the surface of Stone 1  
Q: Quartz, PI: Plagioclase

## X-Ray Powder Diffraction Charts

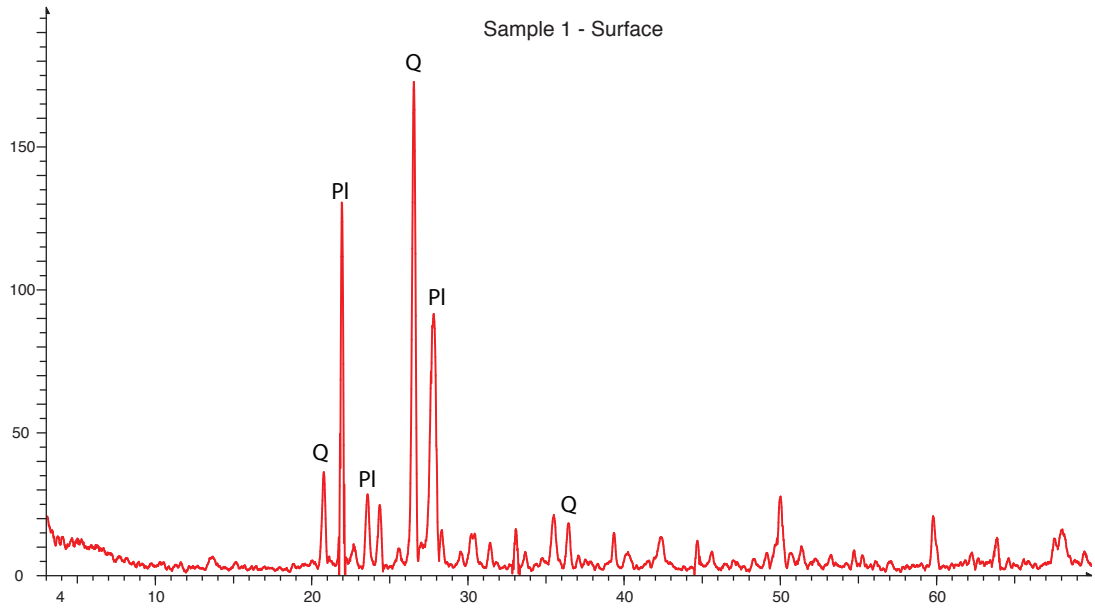


**Figure 35** X-ray diffraction chart for samples collected from the surface of Stone 1  
Q: Quartz, Pl: Plagioclase

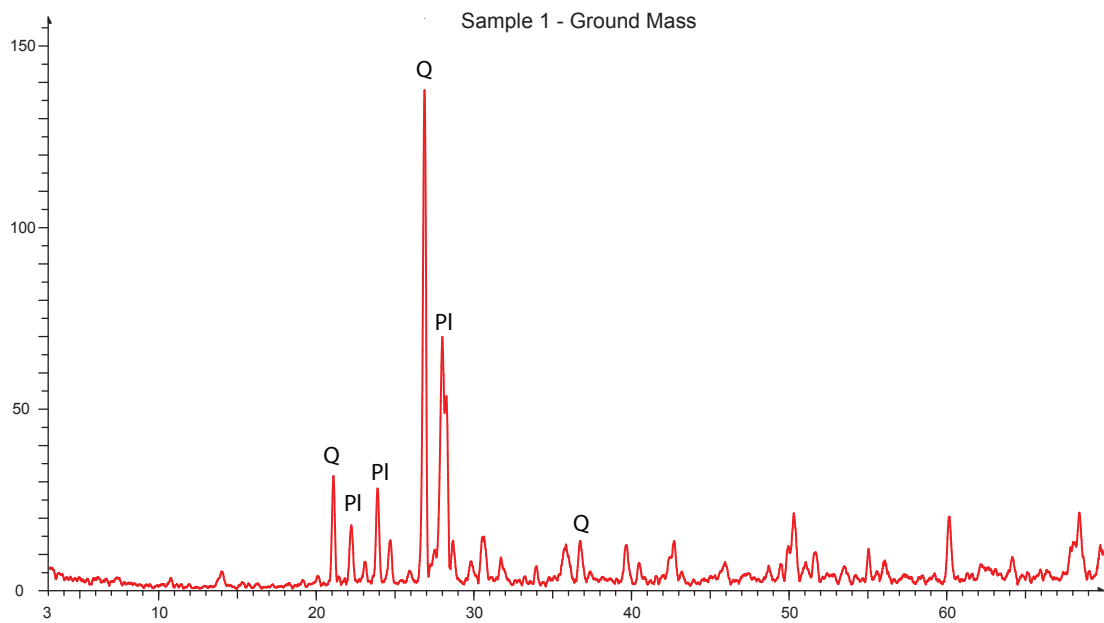


**Figure 36** X-ray diffraction charts for samples collected from the ground mass of Stone 1  
Q: Quartz, Pl: Plagioclase

## X-Ray Powder Diffraction Charts

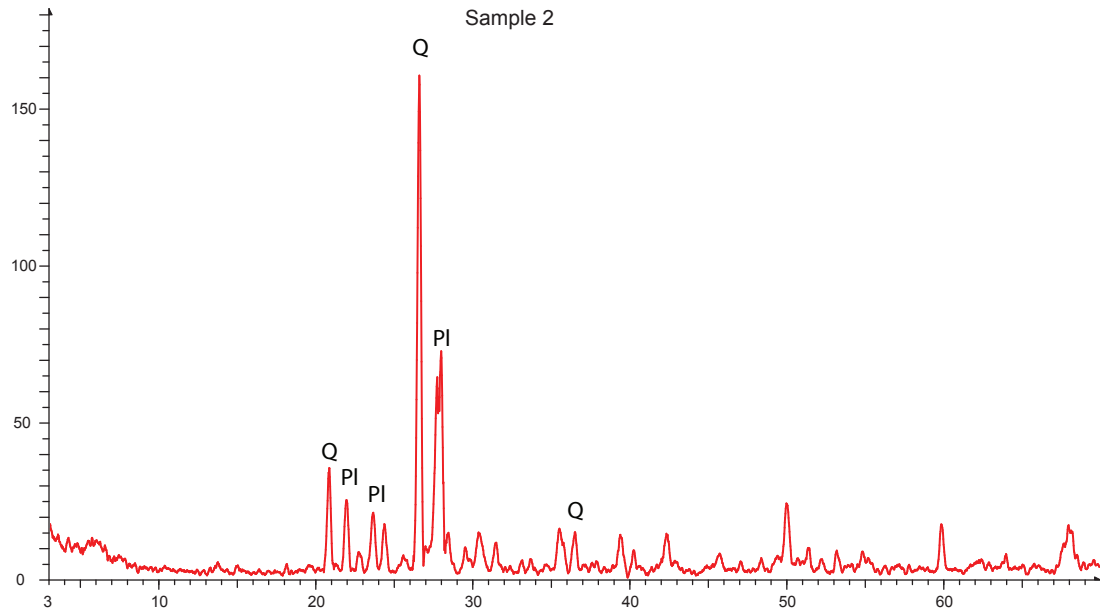


**Figure 37** X-ray diffraction charts for sample collected from the interior parts of Stone 2  
Q: Quartz, Pl: Plagioclase

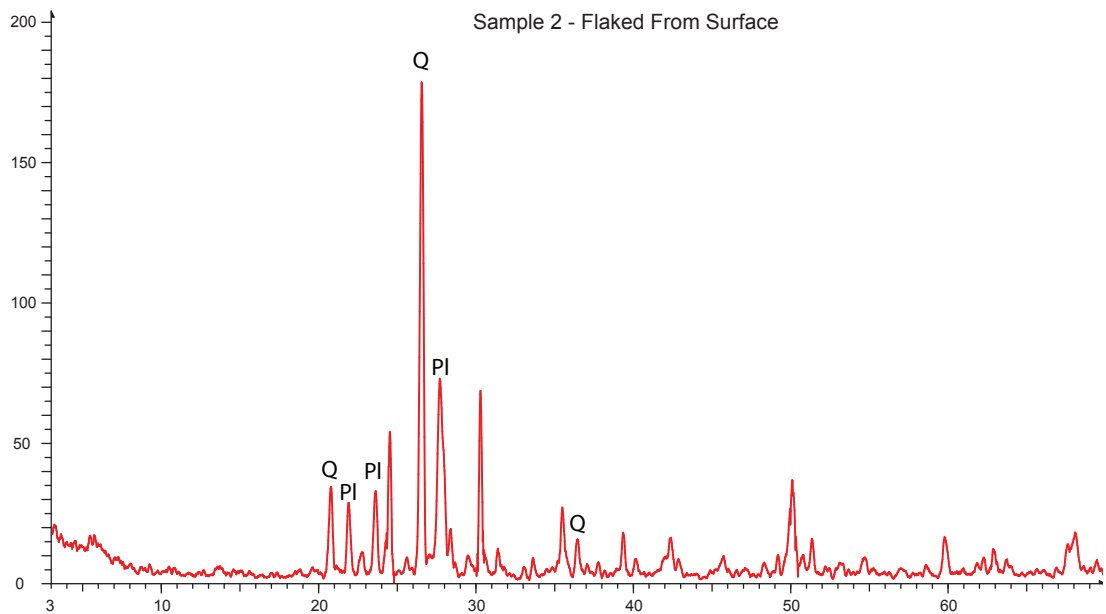


**Figure 38** X-ray diffraction charts for samples collected from the surface of Stone 2  
Q: Quartz, Pl: Plagioclase

## X-Ray Powder Diffraction Charts

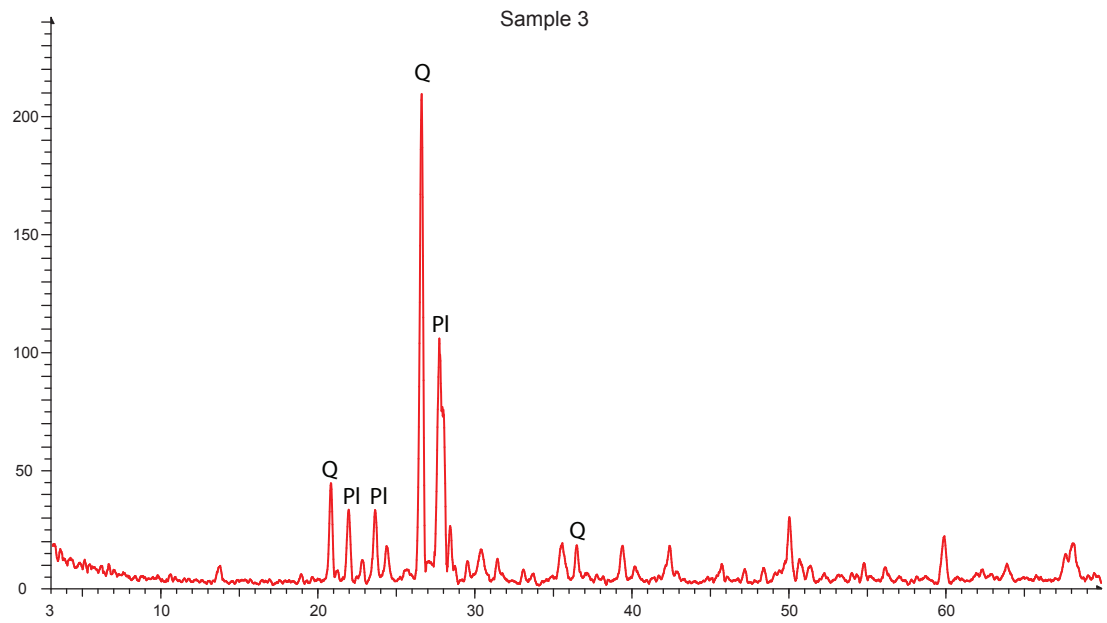


**Figure 39** X-ray diffraction chart for sample collected from the interior parts of Stone 3  
Q: Quartz, Pl: Plagioclase

## X-Ray Powder Diffraction Charts

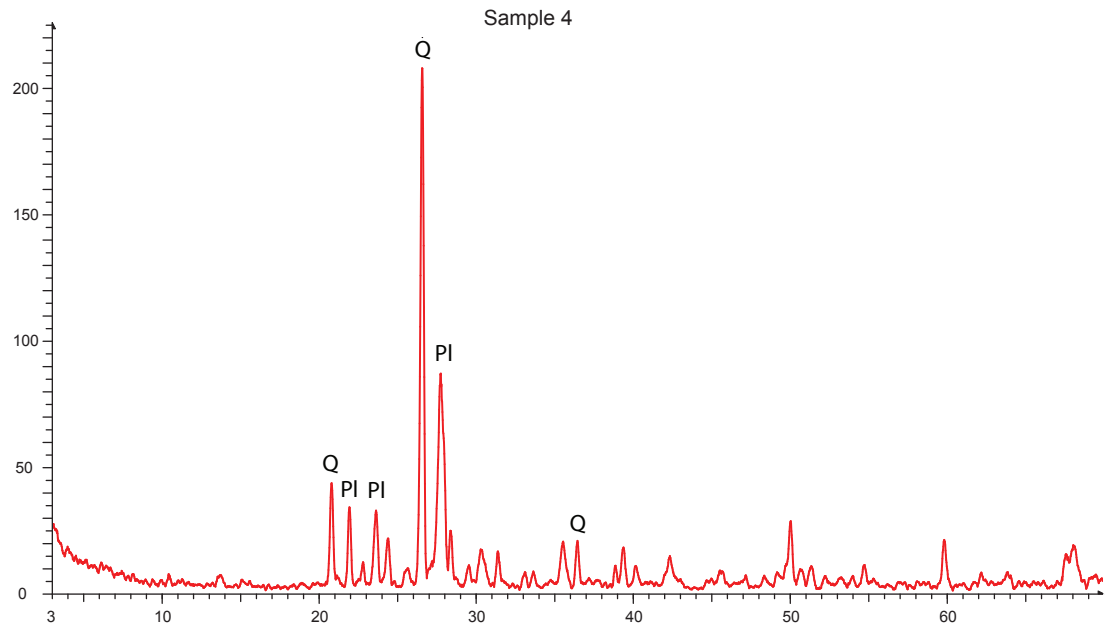


**Figure 40** X-ray diffraction charts for sample collected from the interior parts of Stone 4  
Q: Quartz, Pl: Plagioclase

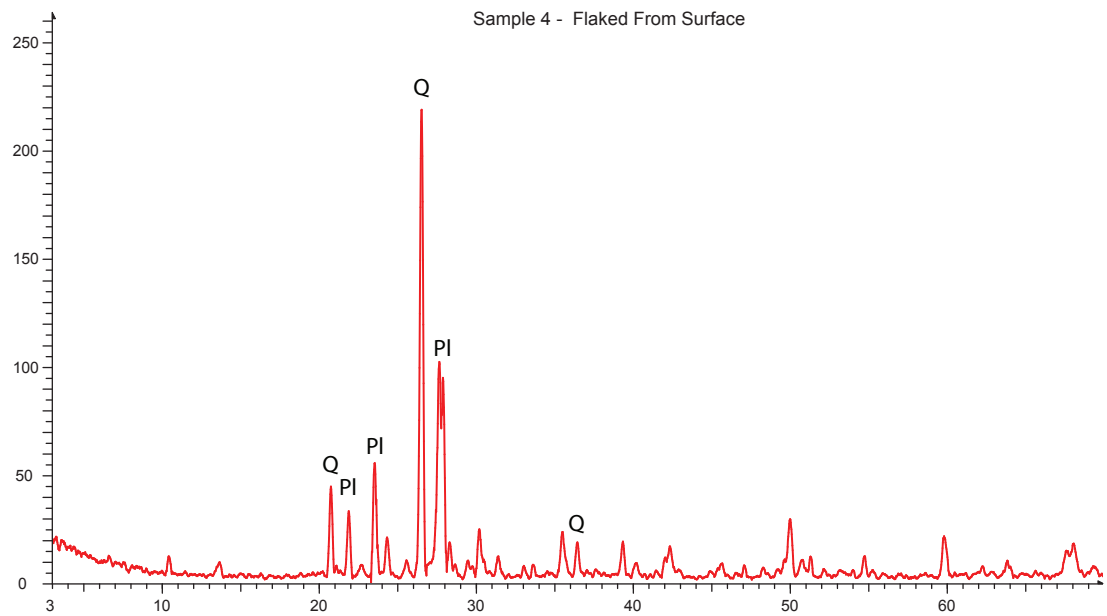


**Figure 41** X-ray diffraction charts for samples collected from the surface of Stone 4  
Q: Quartz, Pl: Plagioclase

## X-Ray Powder Diffraction Charts

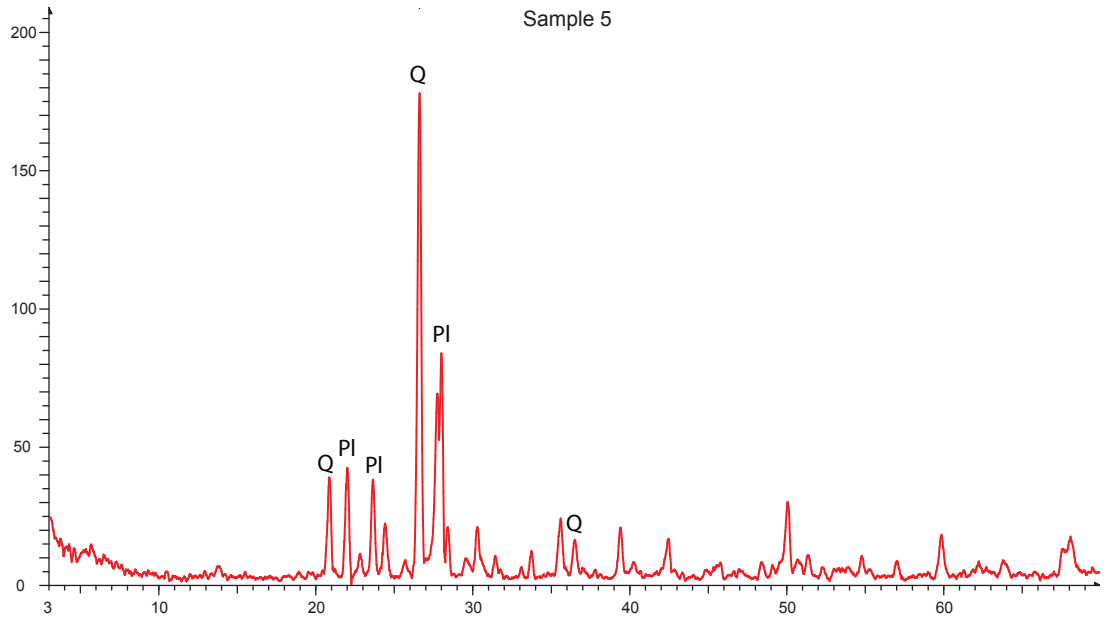


**Figure 42** X-ray diffraction chart for samples collected from the interior parts of Stone 5  
Q: Quartz, PI: Plagioclase

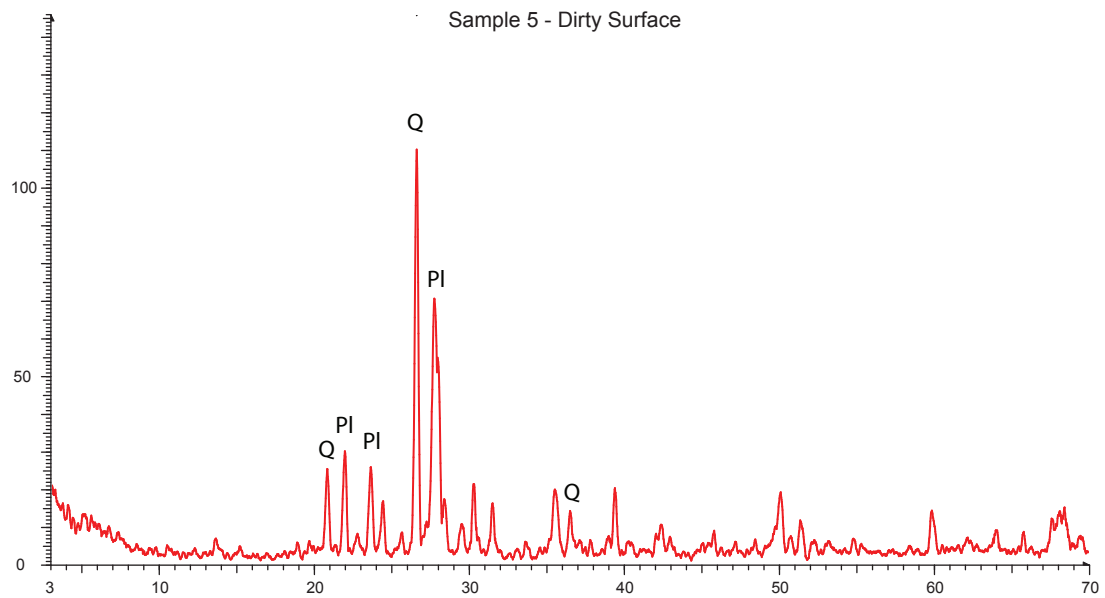


**Figure 43** X-ray diffraction chart for samples collected from the surface of Stone 5  
Q: Quartz, PI: Plagioclase

## Oriented X-Ray Powder Diffraction Charts

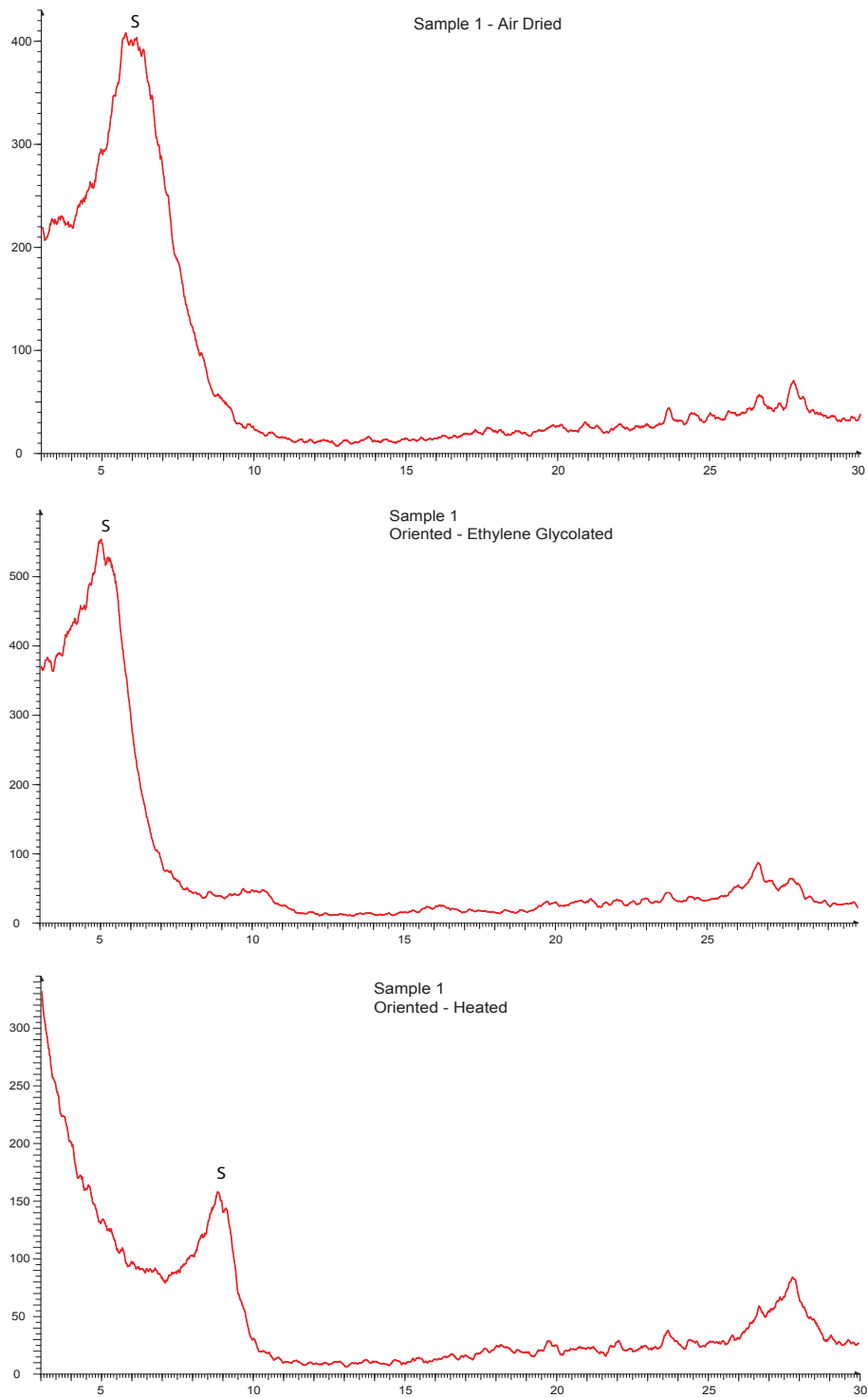


**Figure 44** Oriented X-ray diffraction charts for samples collected from 5 cm beneath the surface of Stone 1.

S: Smectite

## Oriented X-Ray Powder Diffraction Charts

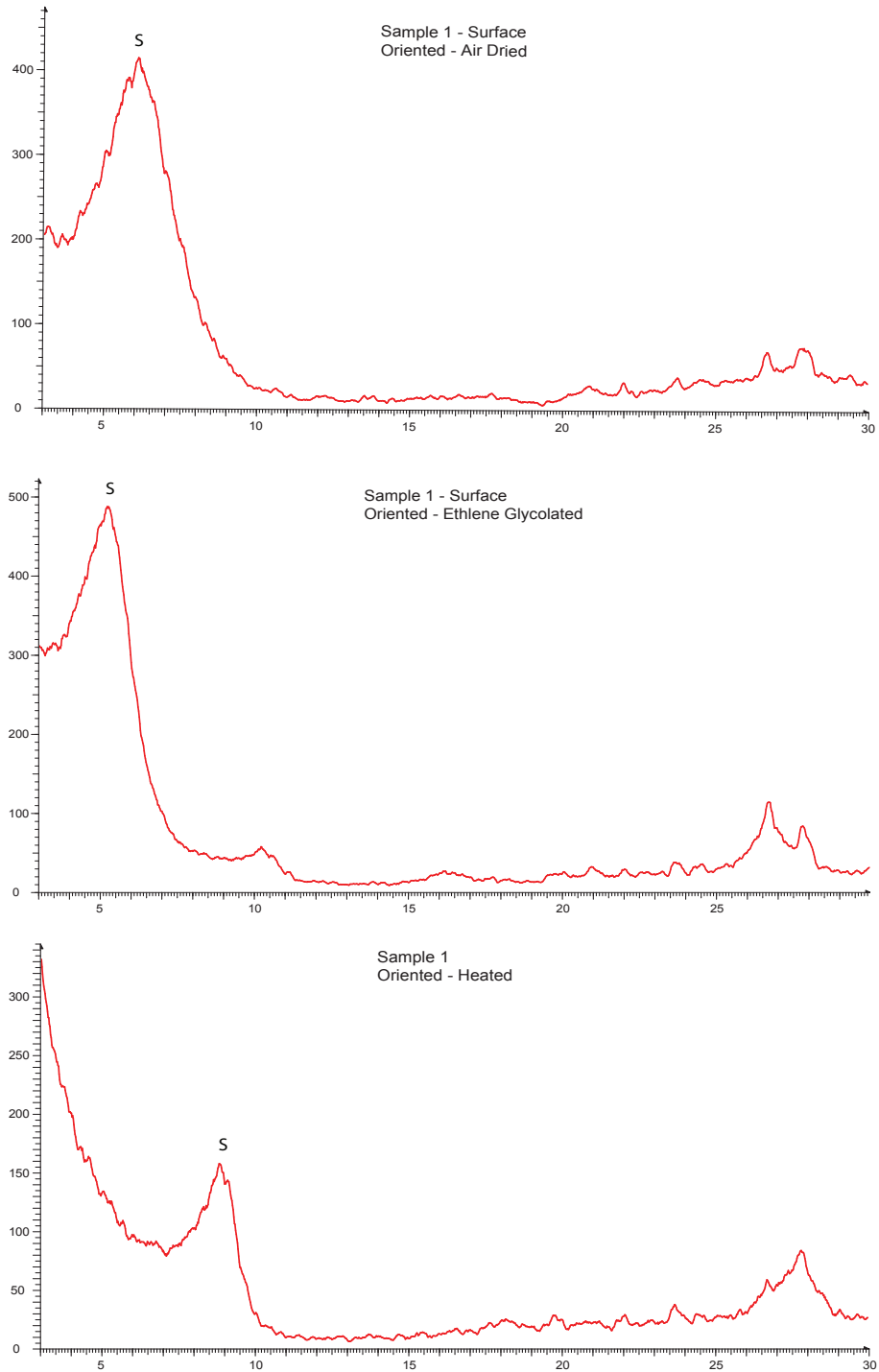


**Figure 45** Oriented X-ray diffraction charts for samples collected from near surface of Stone 1.  
S: Smectite



## Oriented X-Ray Powder Diffraction Charts

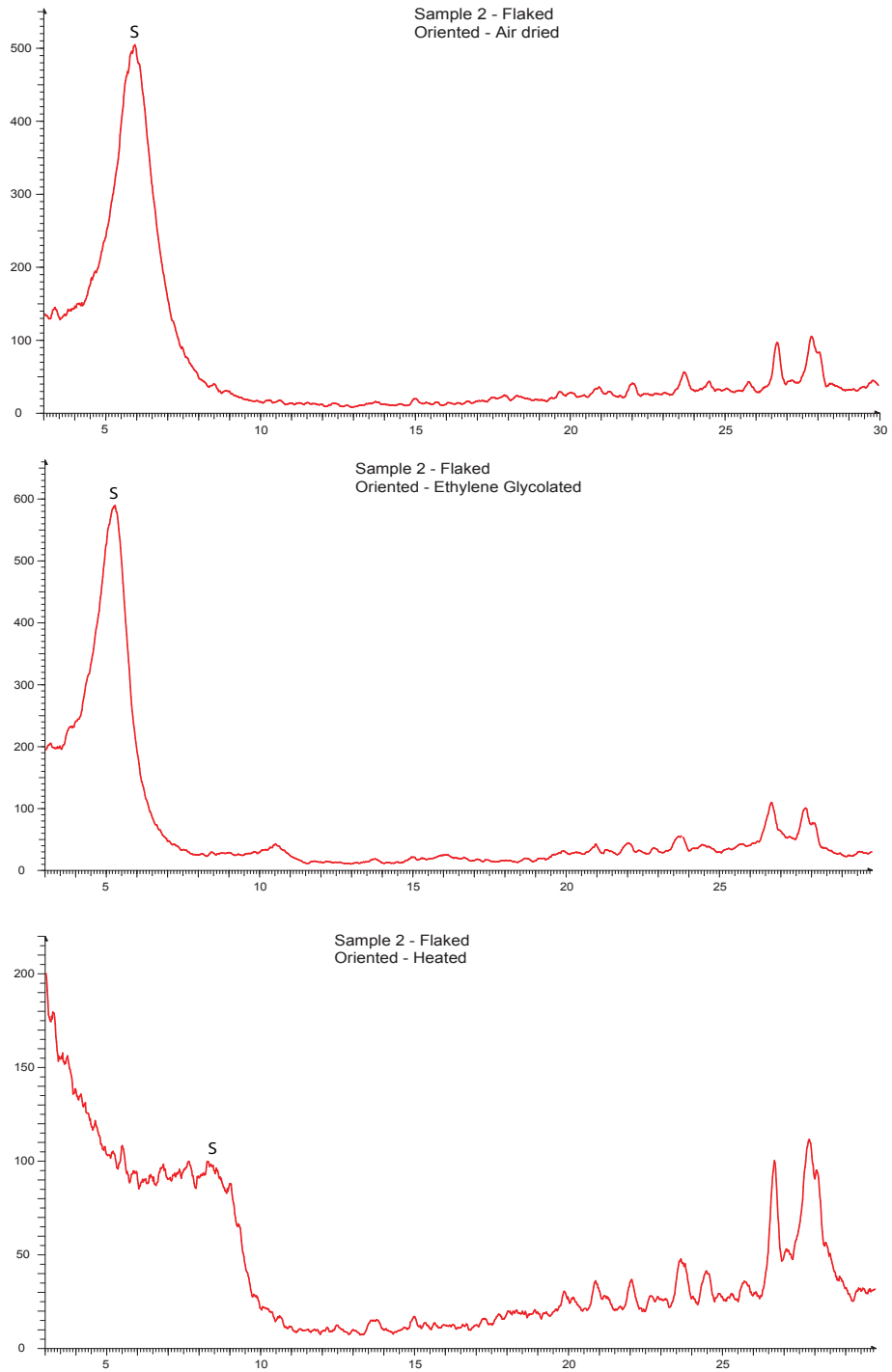


**Figure 46** Oriented X-ray diffraction charts for samples collected from flaked parts of Stone 2.  
S: Smectite

## Oriented X-Ray Powder Diffraction Charts

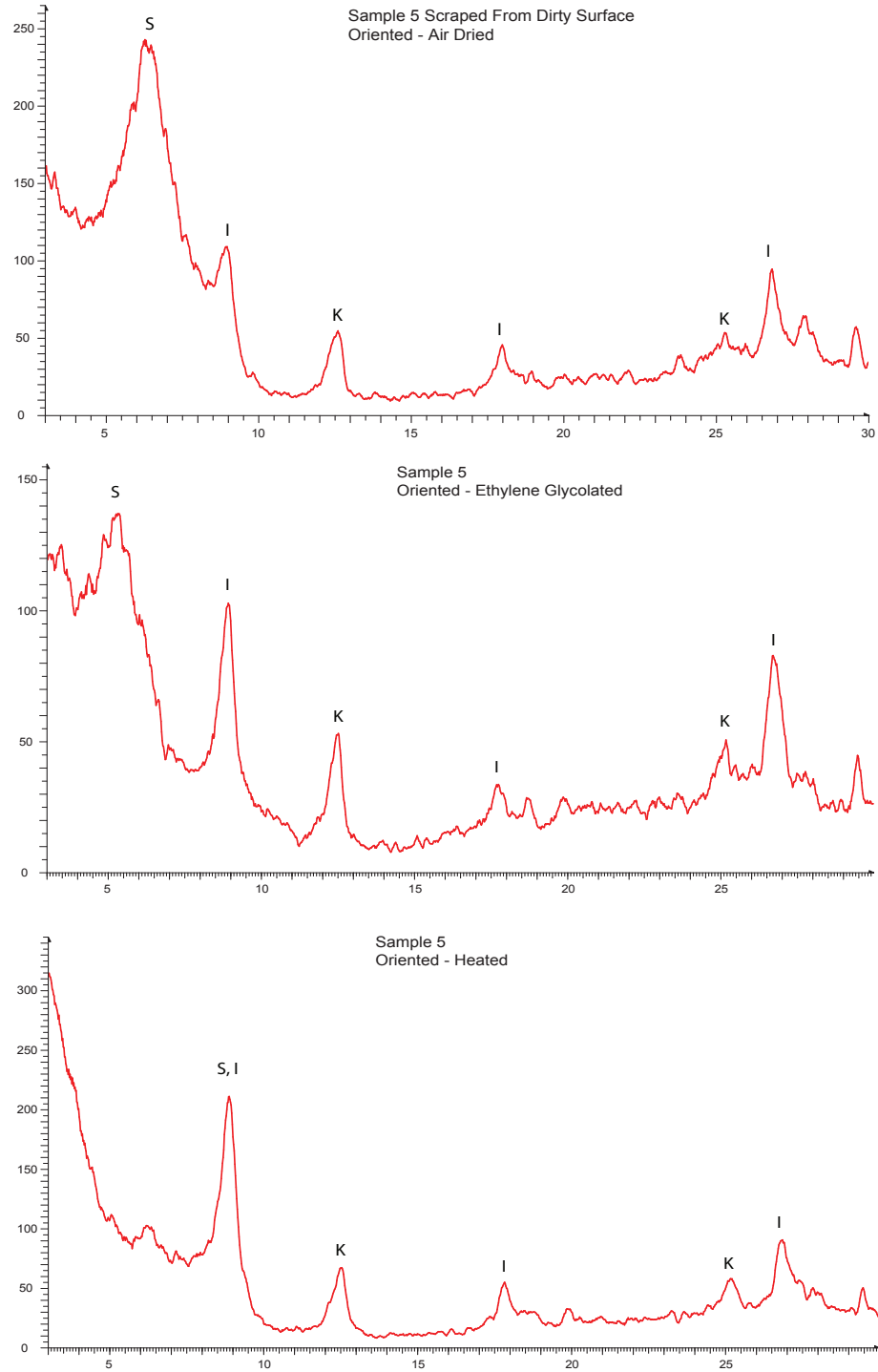


**Figure 47** Oriented X-ray diffraction charts for samples stratched from surface of Stone 5.  
S: Smectite, I: Illite, K: Kaoline